

Performance of the VLT/FORS2 spectropolarimetric mode

Aleksandar Cikota

European Southern Observatory, Germany

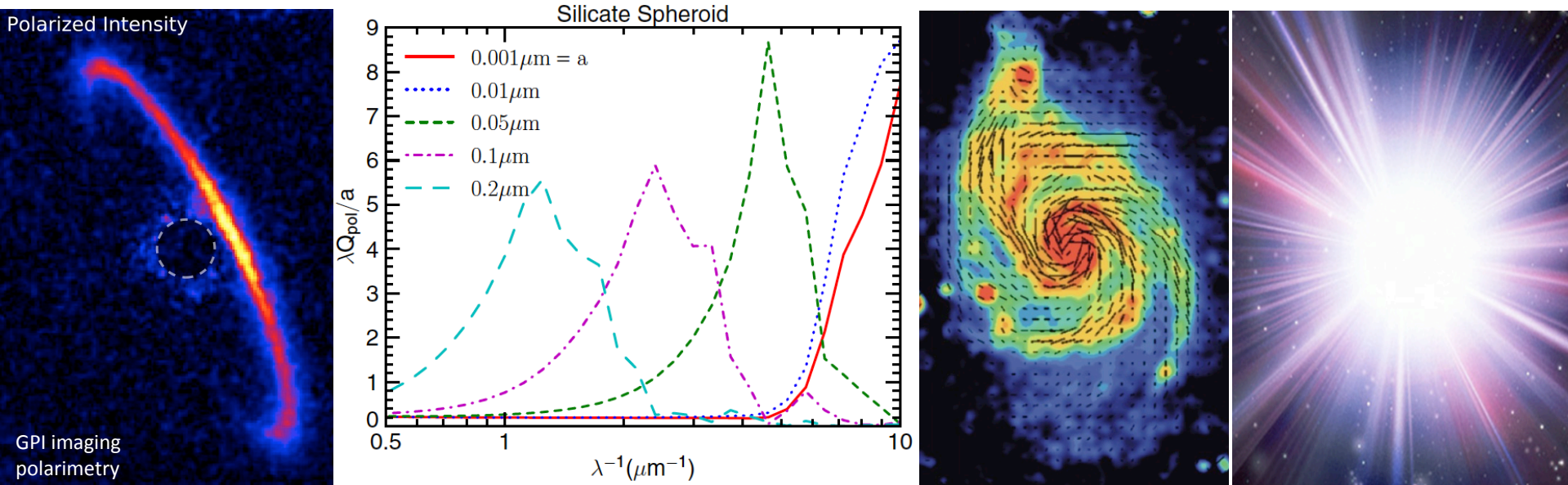
PhD student

Supervisor: Ferdinando Patat

Collaborators: Stefano Bagnulo, Nick Cox, Frans Snik

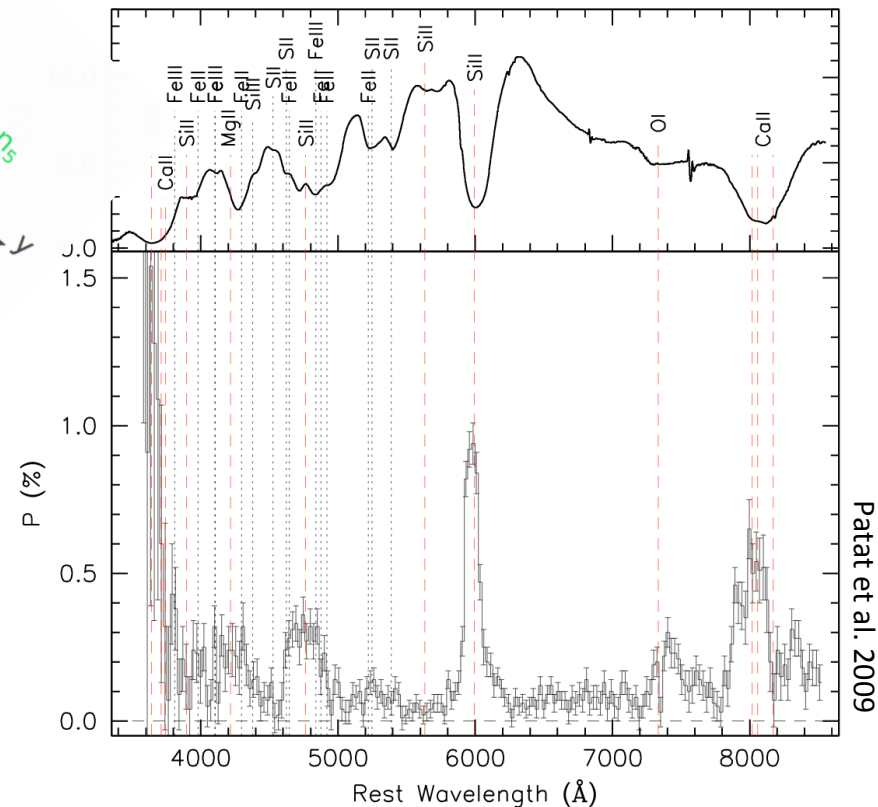
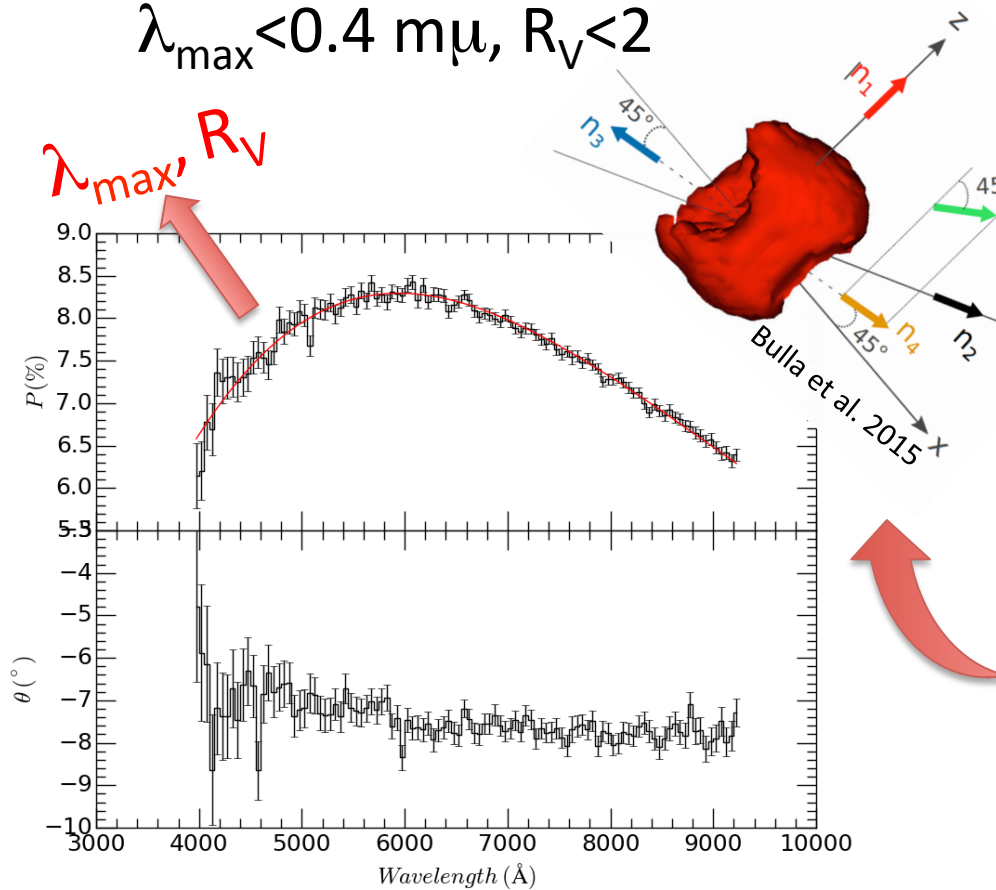
Application of (spectro)polarimetry

- size, shape, orientation, and composition of dust particles
- weak reflected-light signatures (*e.g.*, extra-solar planets)
- scattering properties of light-reflecting screens (*e.g.*, planetary atmospheres, dust shells, surfaces of asteroids)
- magnetic fields (strength and geometry; stellar and galactic)
- 3D shapes of point sources (*e.g.* supernova explosions)



Motivation: ISM & SNe Ia

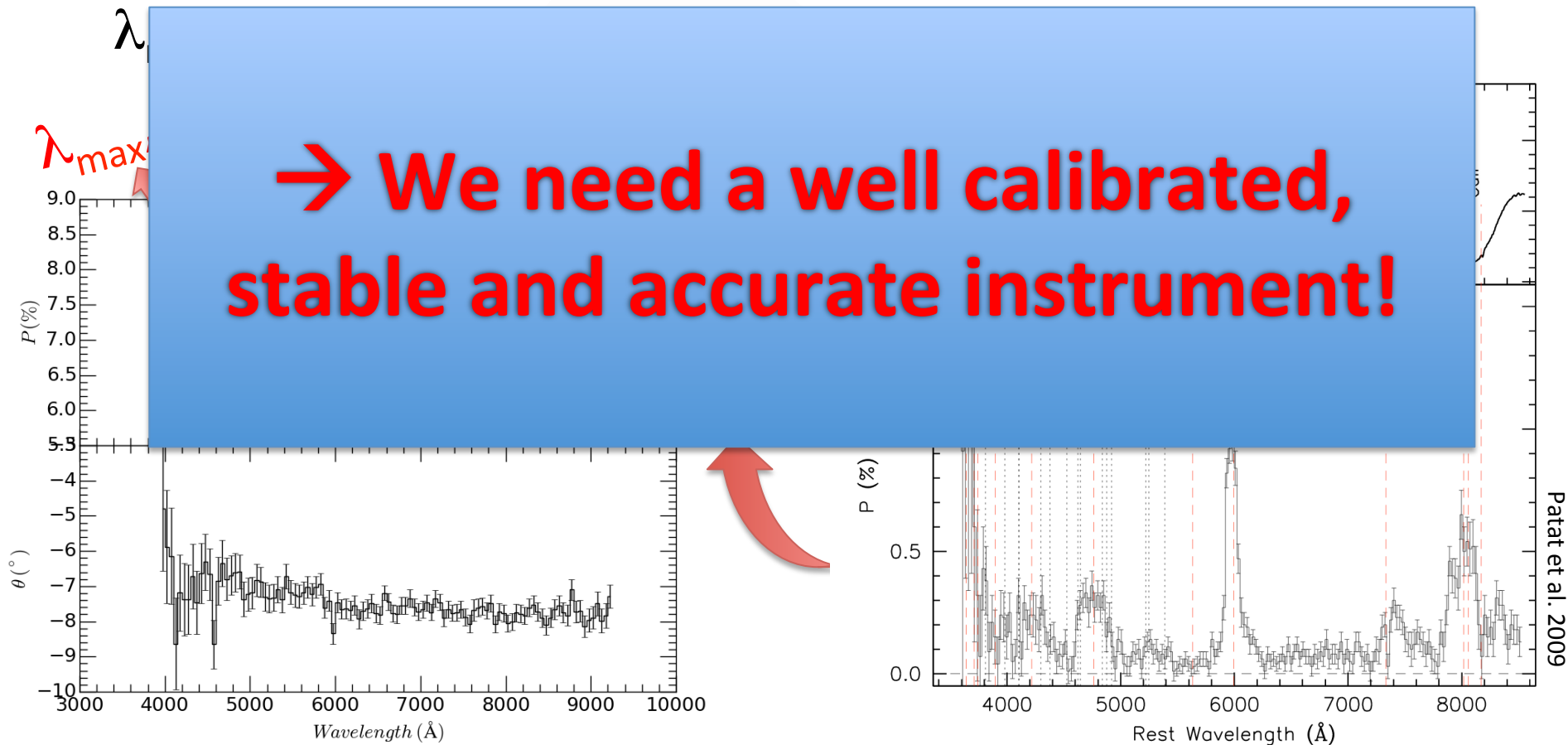
- the progenitor system of SNe Ia is still unknown (SD or DD)
- many SNe Ia demonstrate peculiar dust properties, with,
 $\lambda_{\text{max}} < 0.4 \text{ m}\mu$, $R_V < 2$



Motivation: ISM & SNe Ia

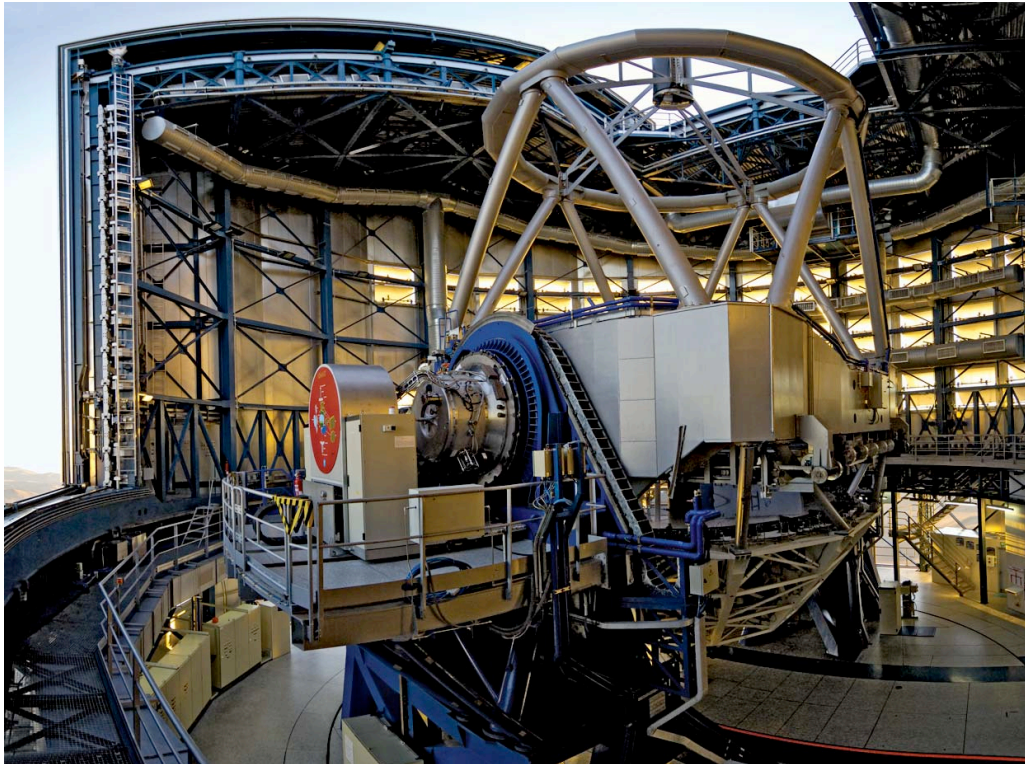
- the progenitor system of SNe Ia is still unknown (SD or DD)
- many SNe Ia demonstrate peculiar dust properties, with,

→ We need a well calibrated, stable and accurate instrument!

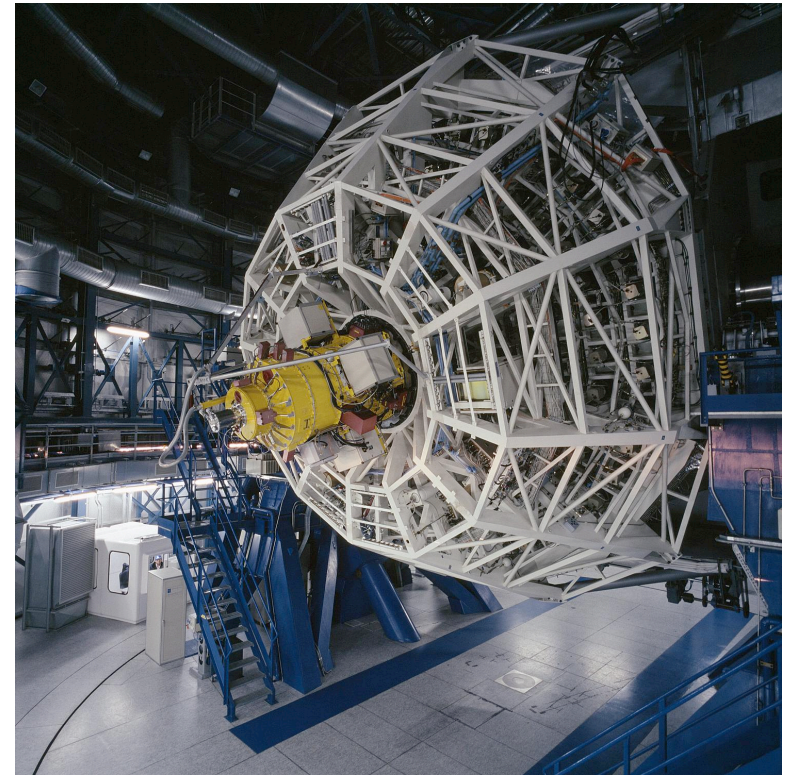


Instrument: FORS2

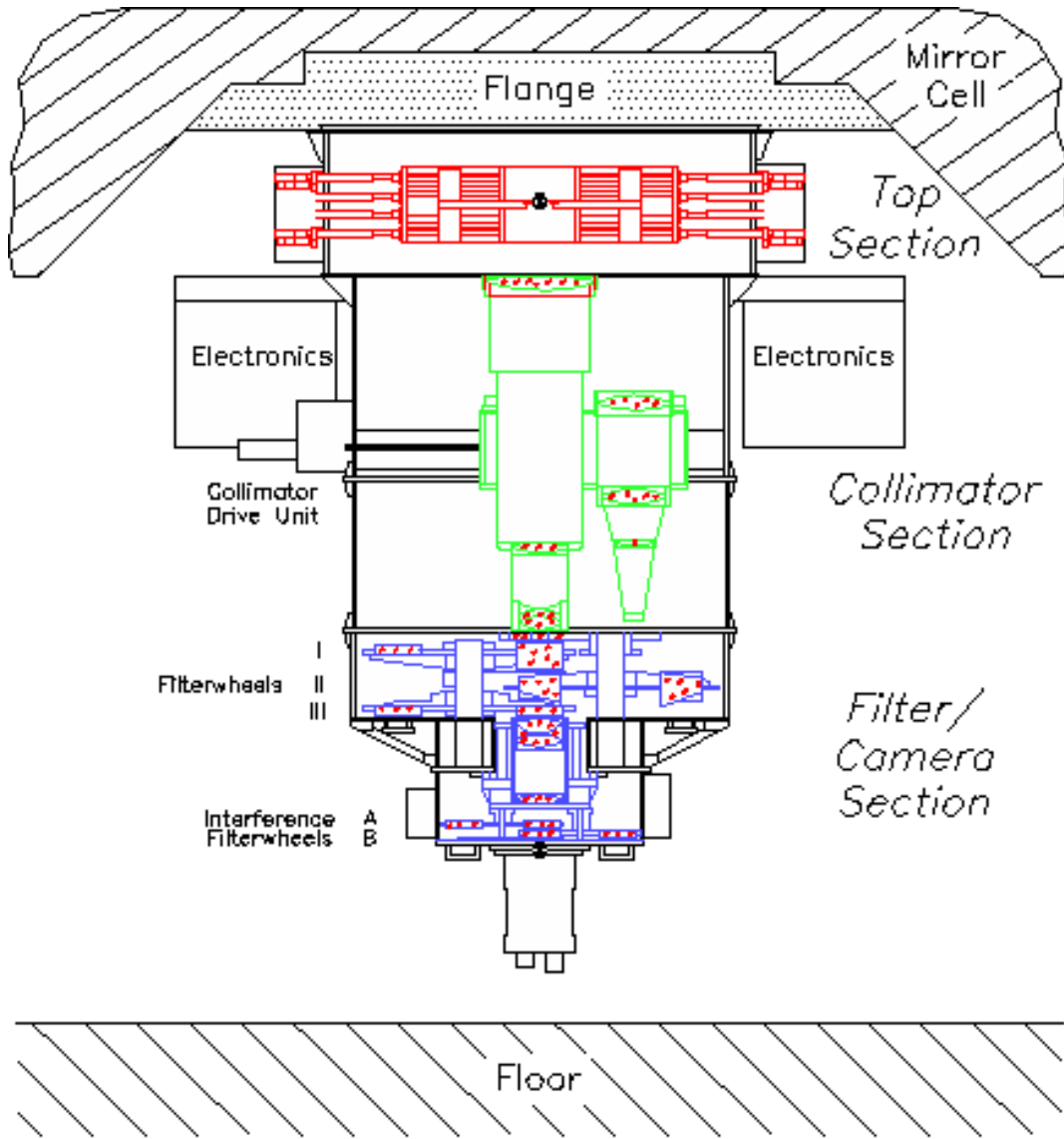
F O cal Reducer/low dispersion Spectrograph 2 (*FORS2*)



UT1 (Antu) of the *Very Large Telescope* (VLT),
Paranal, Chile

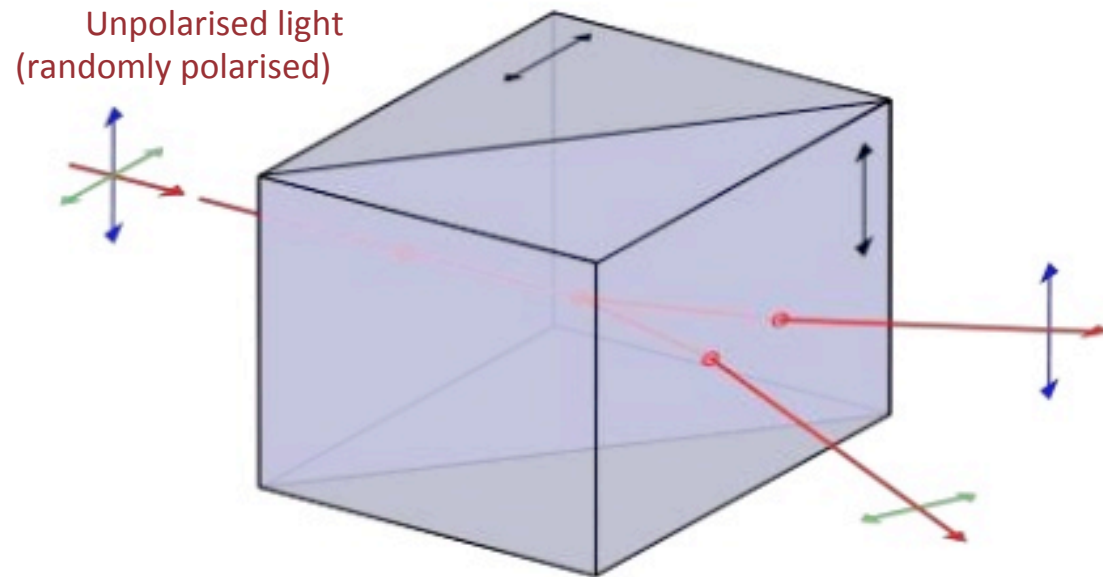
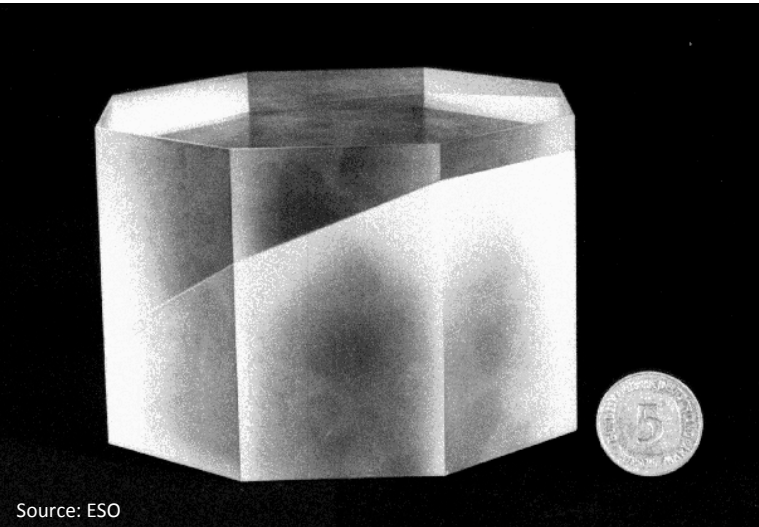


Instrument: FORS2



- Top Section: focal plane equipment, including the multi object spectroscopy (MOS) unit with 19 movable slits, the longslits, the polarimetry mask, the MXU mask exchange unit and the two calibration units.
- The Collimator Section with the two collimators
- The Filter/Camera Section: retarder plate mosaics, the wheel for the Wollaston prism and optional optical analyzers (filters and/or grisms), the grism wheel and the broadband filter wheel in the parallel beam.

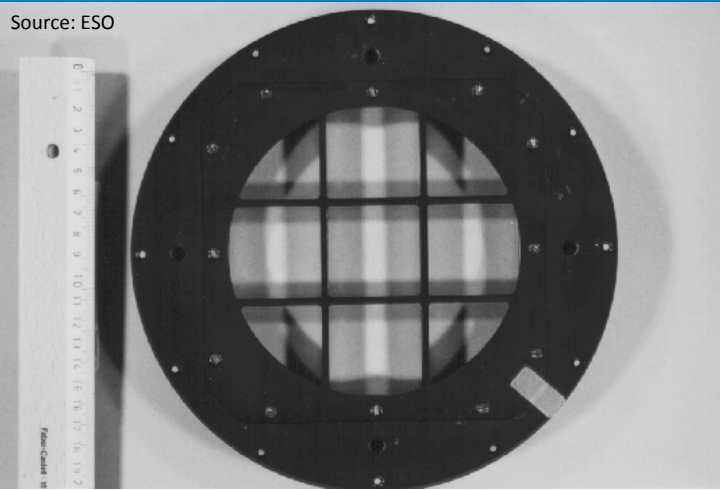
Instrument: Wollaston prism



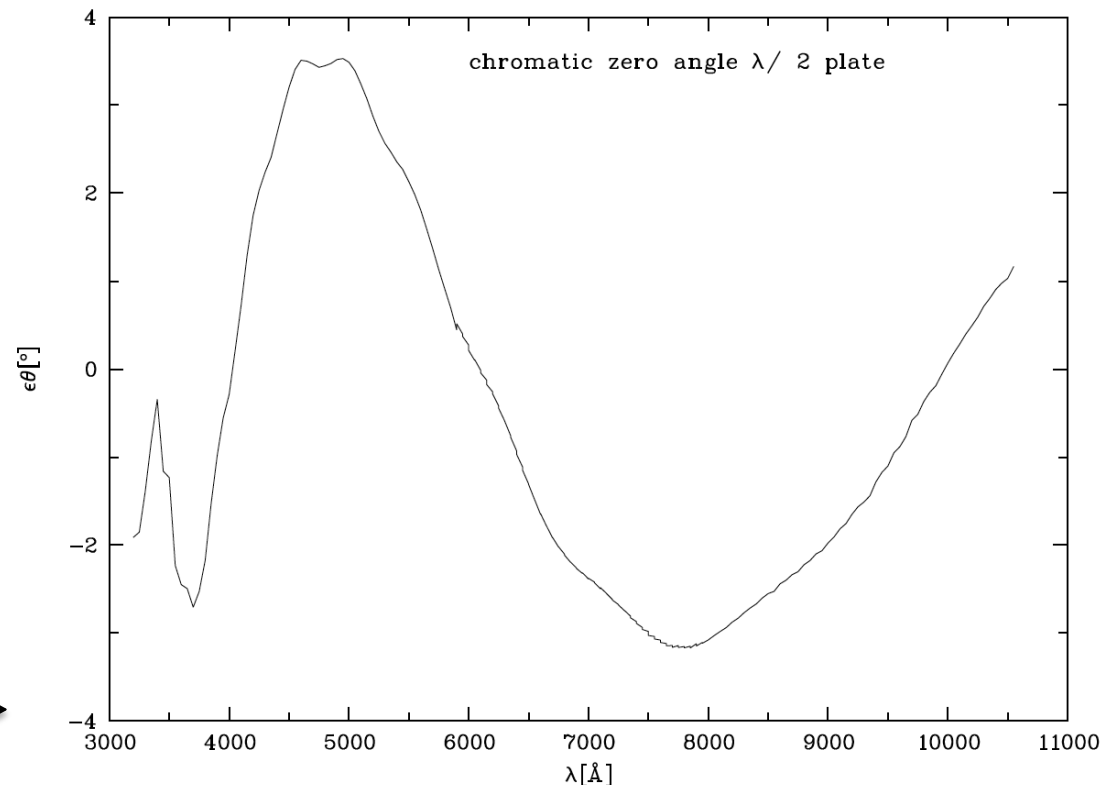
- Made of two layers of crystalline substance, e.g. quartz
- splits the light in two orthogonal polarised outgoing beams (due to variation of refractive index depending on the polarisation of light)

Instrument: Retarder Plate

Source: ESO



Although a super-achromatic half wave plate is used, the the zero angle of the plate is not negligible → all raw measurements of polarization position angles are rotated by an angle of a few degrees.



- impossible to procure waveplates of sufficient size; → mosaics of 3*3 plates of 45.5*45.5mm each are used (inter-plate gap 3mm) with a resulting free mosaic diameter of 138mm.
- "The position angles can be set with an accuracy of 0.1 degree."

Amount of chromatism of the $\lambda/2$ plate, measured with a Glan Thomsen Prism. ►

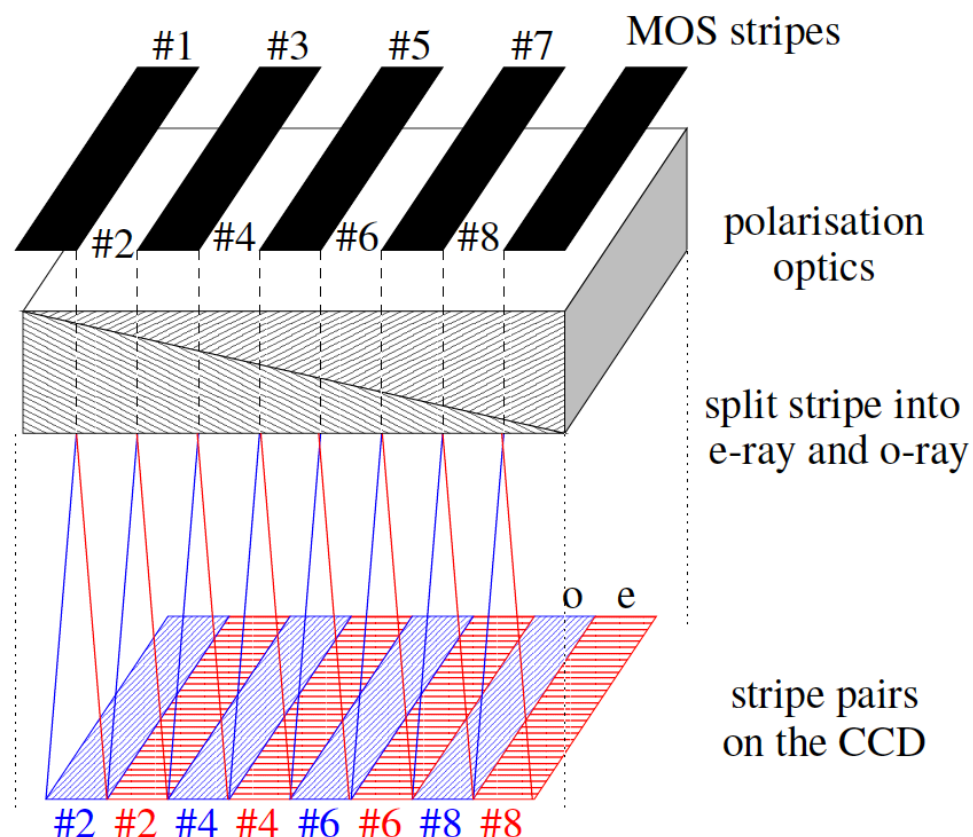
Spectropolarimetry — PMOS mode

MOS Slit/Strip Mask for Spectropolarimetry PMOS: possible with the standard resolution collimator only. The MOS slitlet arms with odd numbers are positioned to form the same strip mask.

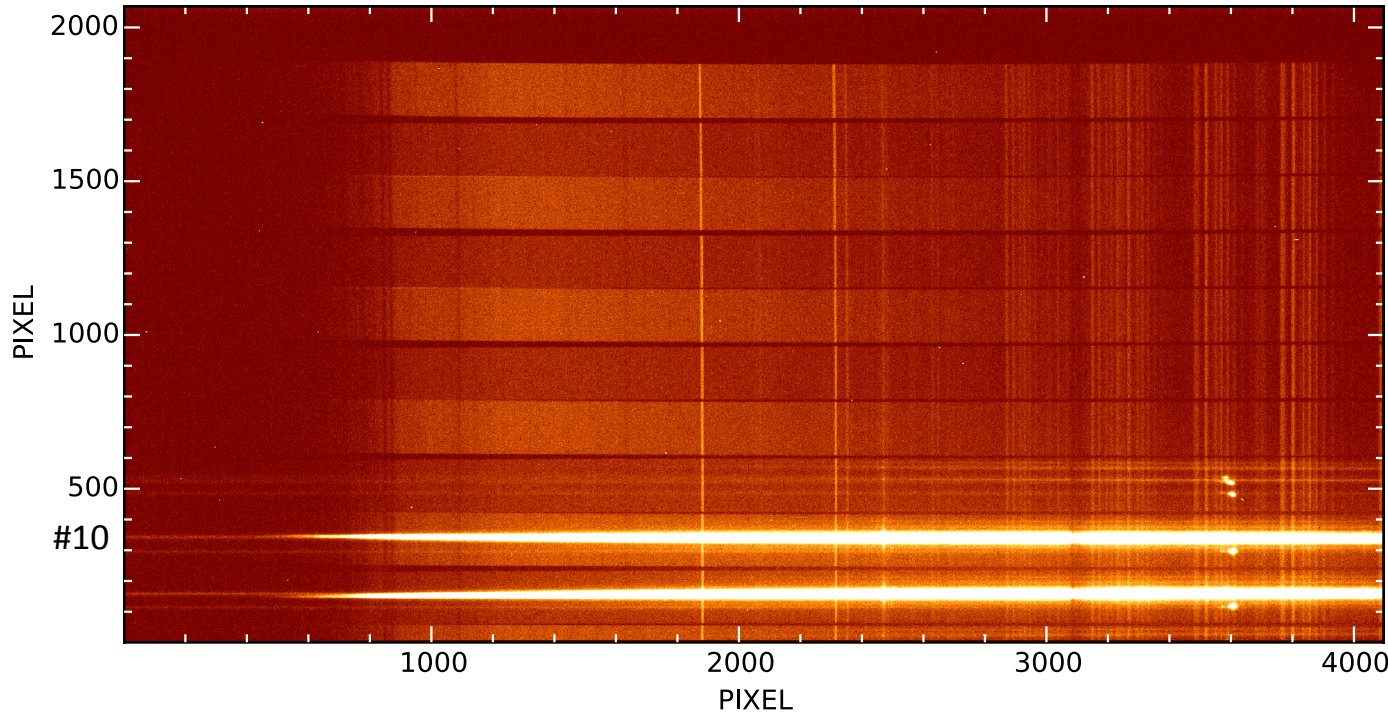
Grisms and Filters for PMOS: all grisms and filters except the few ones mounted on the same wheel as the Wollaston prism. We use **GRIS_300V**, without any filters.

Retarder Plate Angles: can be selected from a set of fixed predefined angles ($\theta_n = n * 22.5^\circ$). We use $\theta = 0, 22.5, 45, 67.5$ degrees.

Acquisition: the selected object is put on MOS slit 10 in the center of the field.



Observations and methods



FORS2: halfwave retarder plate (at angles of 0, 22.5, 45, and 67.5 deg) in front of a Wollaston prism.

- ordinary and
- extraordinary beam, separated by 22''

Stokes
parameters

$$Q = \frac{2}{N} \sum_{i=0}^{N-1} F(\theta_i) \cos(4\theta_i)$$

$$U = \frac{2}{N} \sum_{i=0}^{N-1} F(\theta_i) \sin(4\theta_i)$$

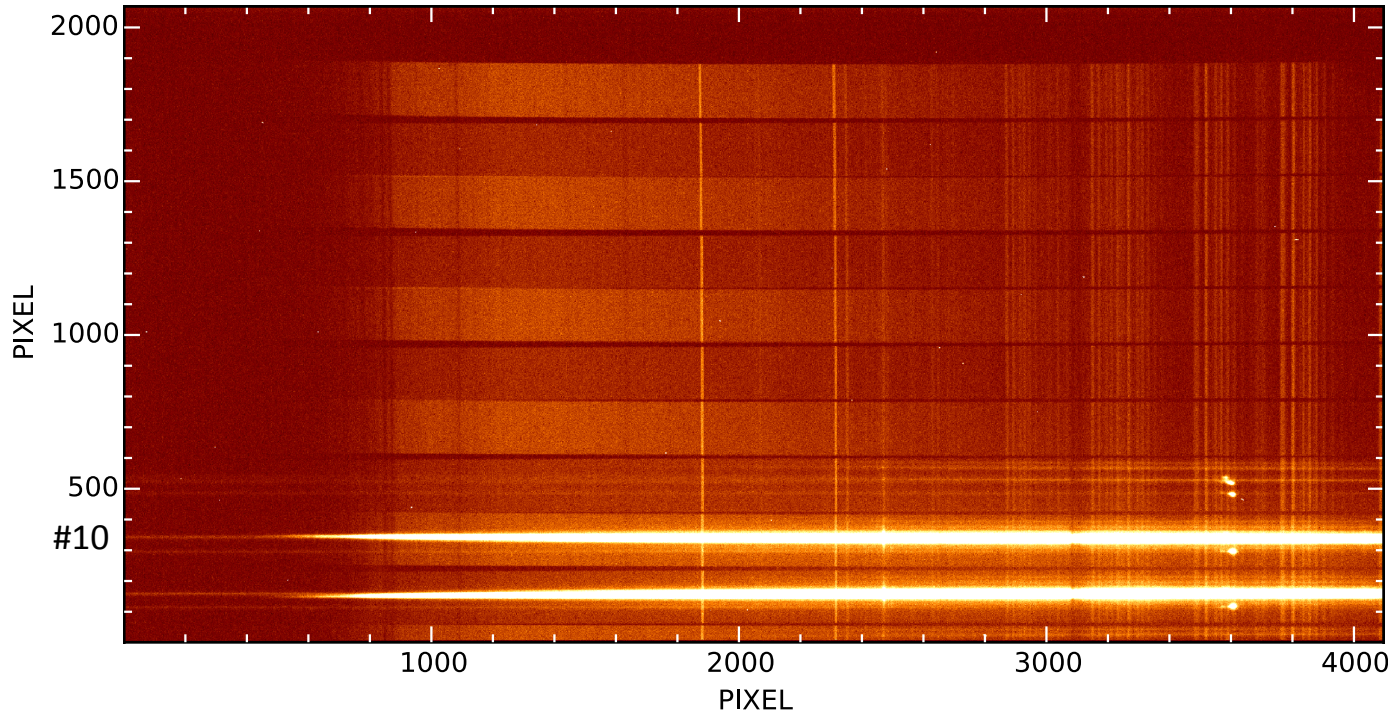
$$P = \sqrt{Q^2 + U^2}$$

Normalized flux
differences

$$F(\theta_i) = \frac{f^o(\theta_i) - f^e(\theta_i)}{f^o(\theta_i) + f^e(\theta_i)}$$

$$\theta_0 = \frac{1}{2} \arctan(U_0/Q_0)$$

Observations and methods



FORS2: halfwave retarder plate (at angles of 0, 22.5, 45, and 67.5 deg) in front of a Wollaston prism.

- ordinary and
- extraordinary beam,
separated by 22''

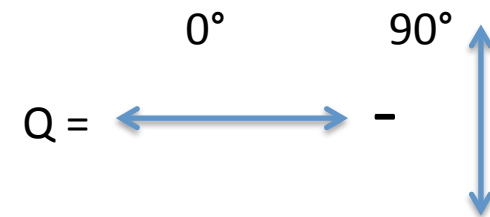
Stokes
parameters

$$Q = \frac{2}{N} \sum_{i=0}^{N-1} F(\theta_i) \cos(4\theta_i)$$

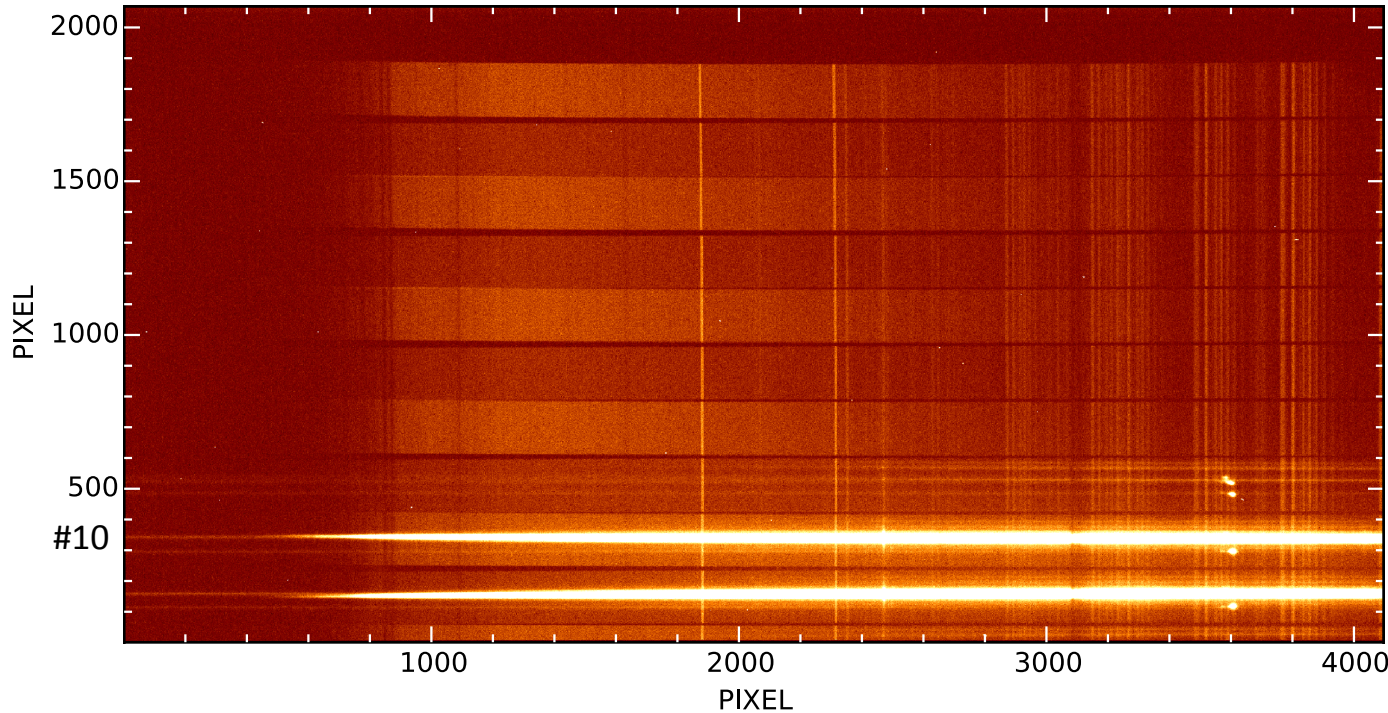
$$U = \frac{2}{N} \sum_{i=0}^{N-1} F(\theta_i) \sin(4\theta_i)$$

Normalized flux
differences

$$F(\theta_i) = \frac{f^o(\theta_i) - f^e(\theta_i)}{f^o(\theta_i) + f^e(\theta_i)}$$



Observations and methods



FORS2: halfwave retarder plate (at angles of 0, 22.5, 45, and 67.5 deg) in front of a Wollaston prism.

- ordinary and
- extraordinary beam, separated by 22"

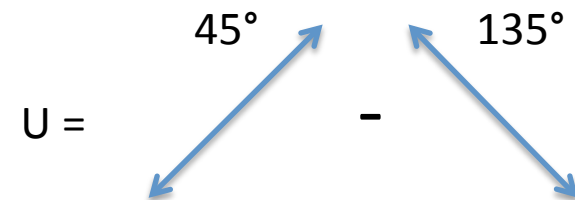
Stokes
parameters

$$Q = \frac{2}{N} \sum_{i=0}^{N-1} F(\theta_i) \cos(4\theta_i)$$

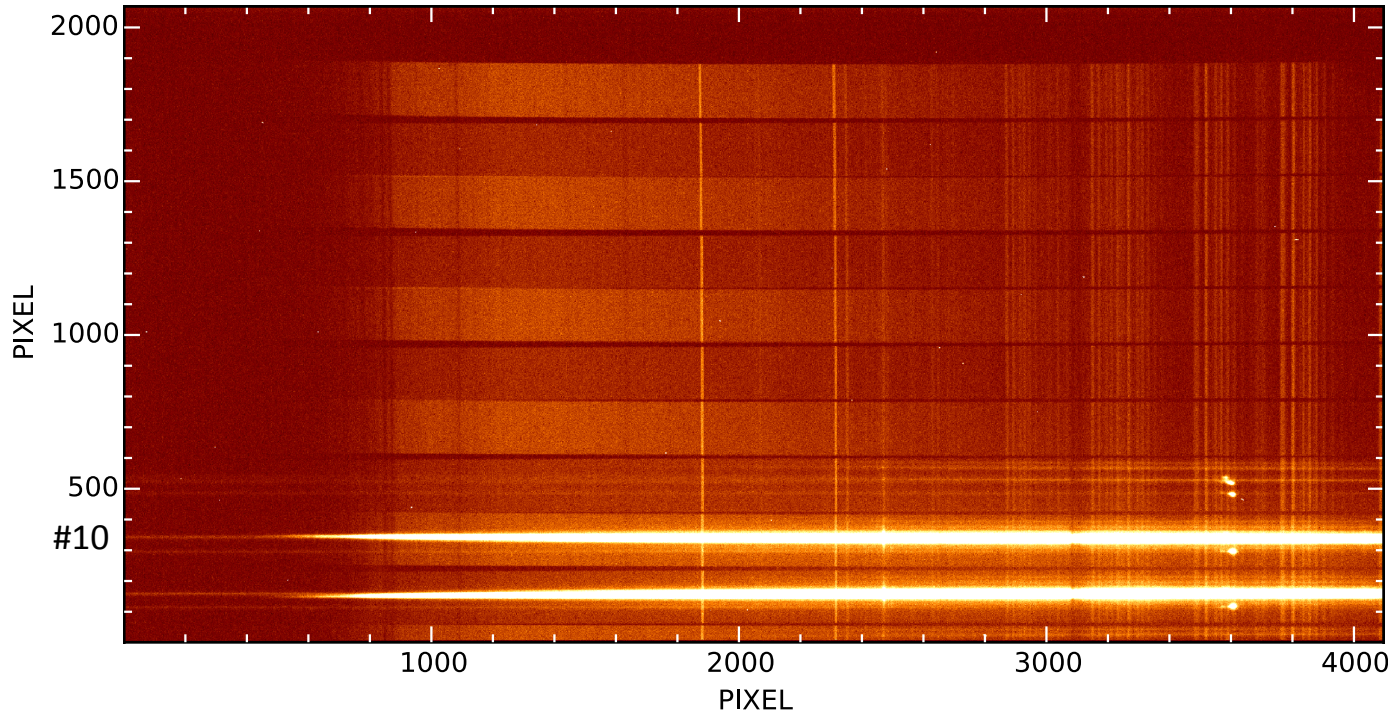
$$U = \frac{2}{N} \sum_{i=0}^{N-1} F(\theta_i) \sin(4\theta_i)$$

Normalized flux
differences

$$F(\theta_i) = \frac{f^o(\theta_i) - f^e(\theta_i)}{f^o(\theta_i) + f^e(\theta_i)}$$



Observations and methods



FORS2: halfwave retarder plate (at angles of 0, 22.5, 45, and 67.5 deg) in front of a Wollaston prism.

- ordinary and
- extraordinary beam, separated by 22''

Stokes
parameters

$$Q = \frac{2}{N} \sum_{i=0}^{N-1} F(\theta_i) \cos(4\theta_i)$$

$$U = \frac{2}{N} \sum_{i=0}^{N-1} F(\theta_i) \sin(4\theta_i)$$

$$P = \sqrt{Q^2 + U^2}$$

Normalized flux
differences

$$F(\theta_i) = \frac{f^o(\theta_i) - f^e(\theta_i)}{f^o(\theta_i) + f^e(\theta_i)}$$

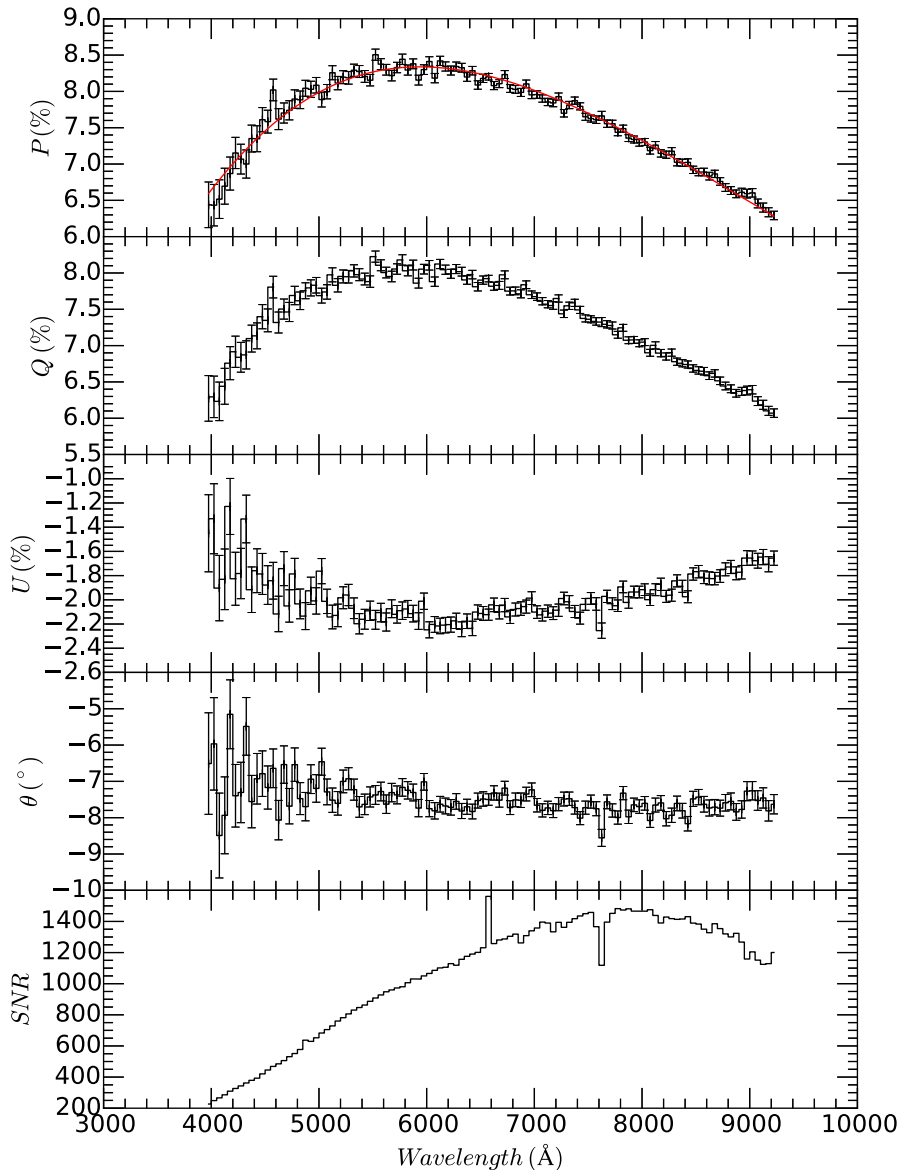
$$\theta_0 = \frac{1}{2} \arctan(U_0/Q_0)$$

Stars sample

- Selected from: FORS Standard fields and Stars list
- 6 polarized standards at 30 epochs, 8 unpolarized standards at 40 epoch
- Observed between 2009 and 2016

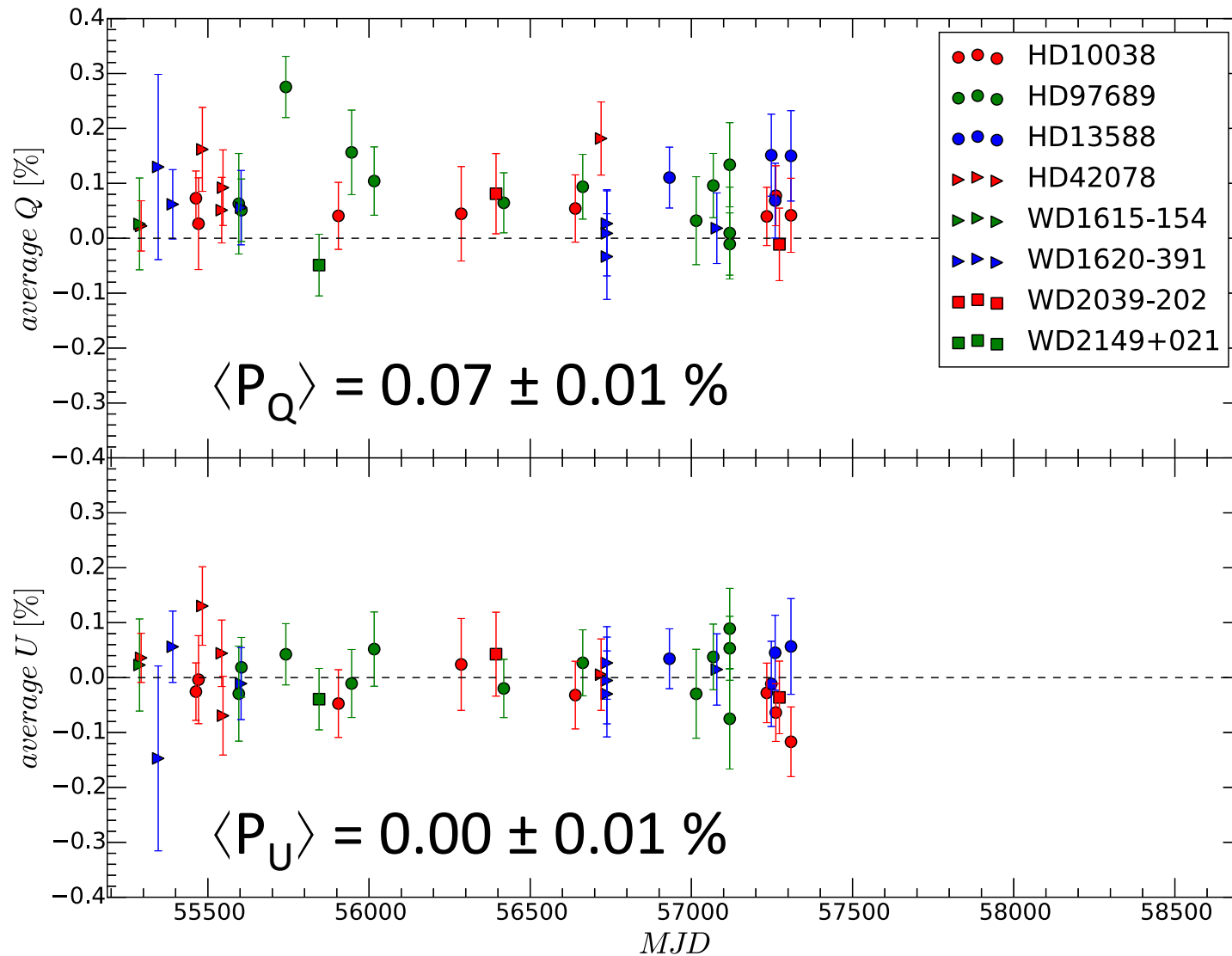
Name	V mag	Spec. Type	Type	No. of epochs
HD 10038	8.1	A2mA5-F0	unPol.	8
HD 13588	7.9	A1m	unPol.	4
HD 42078	6.2	Am	unPol.	5
HD 97689	6.8	A0m	unPol.	12
WD 1615-154	13.4	DA1.7	unPol.	1
WD 1620-391	11.0	DA2	unPol.	7
WD 2039-202	12.4	DA2.5	unPol.	2
WD 2149+021	12.7	DA2.8	unPol.	1
NGC 2024 1	12.2	B0.5V	Pol.	7
Vela1 95	12.1	OB+	Pol.	11
Hiltner 652	10.8	B1II-III	Pol.	8
HDE 316232	10.4	O9IV	Pol.	1
BD -14 4922	9.73	O9.5	Pol.	2
BD -12 5133	10.4	B1V	Pol.	1

Results



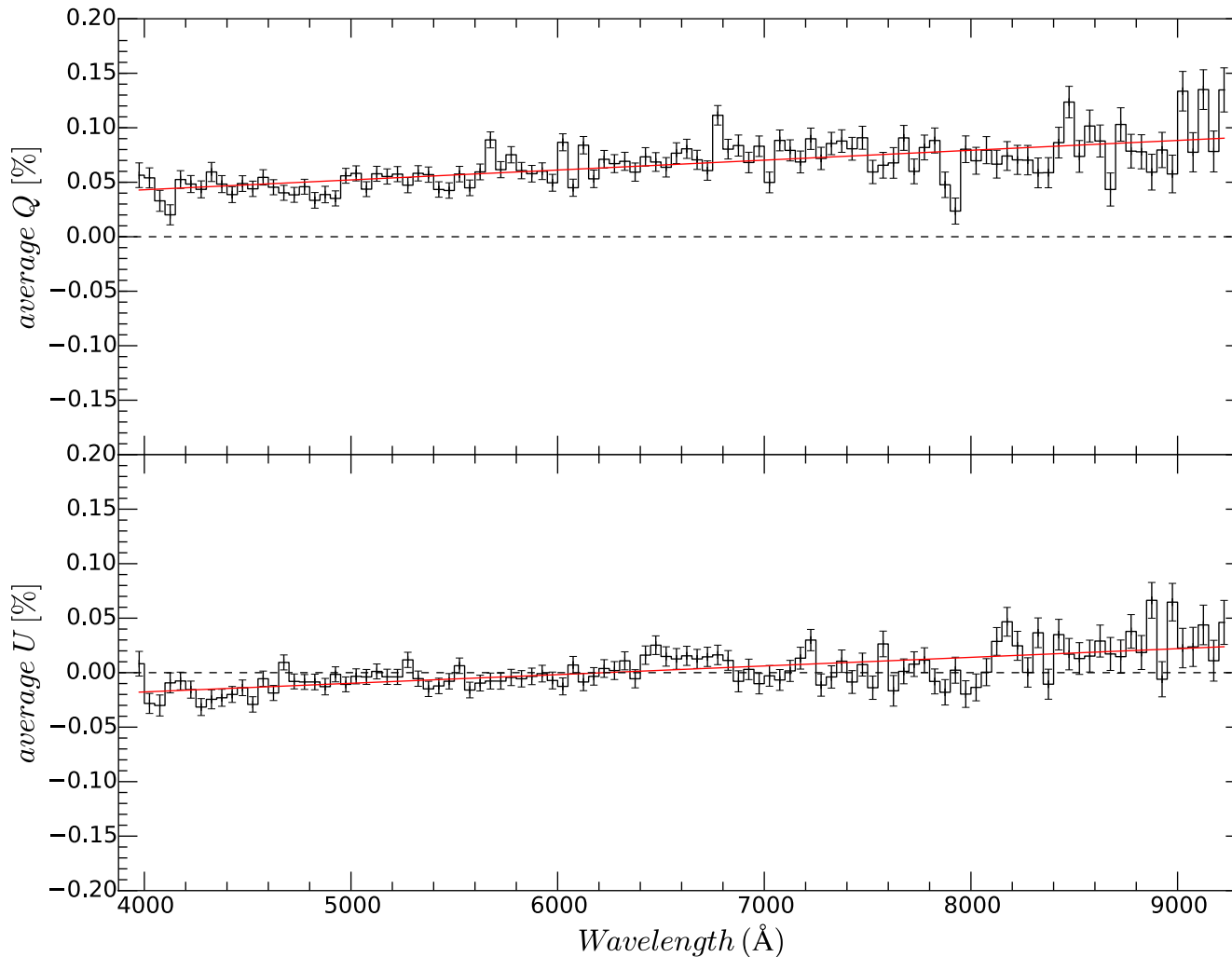
- Wavelength ranges from 3950-9300Å
- Binned in 50Å bins
- SNR typically between 500-2000 per 50Å bin
- We also calculate the polarization in Bessel's *BVRI* passbands

Results: unpolarized stars



Results: unpolarized stars

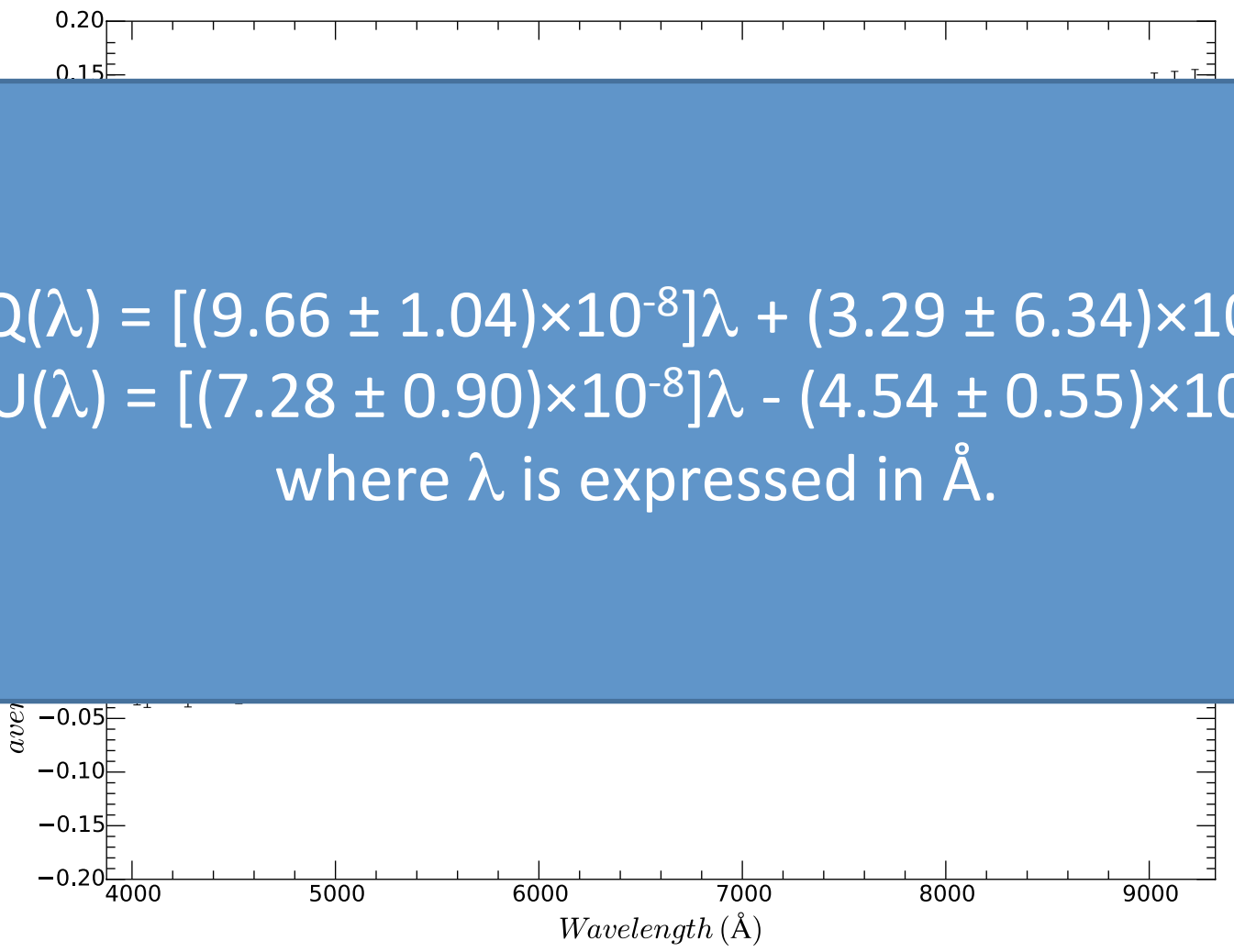
- weighted mean of all 40 epochs



Cikota et al. 2017

Results: unpolarized stars

- weighted mean of all 40 epochs


$$Q(\lambda) = [(9.66 \pm 1.04) \times 10^{-8}] \lambda + (3.29 \pm 6.34) \times 10^{-5}$$
$$U(\lambda) = [(7.28 \pm 0.90) \times 10^{-8}] \lambda - (4.54 \pm 0.55) \times 10^{-4}$$

where λ is expressed in \AA .

Linear spectropolarimetry of polarimetric standard stars with VLT/FORS2

Aleksandar Cikota,¹★ Ferdinando Patat,¹ Stefan Cikota² and Tamar Faran¹

¹*European Southern Observatory, Karl-Schwarzschild-Str 2, D-85748 Garching b. München, Germany*

²*Physics Department, University of Split, Ruđera Boškovića 33, 21000 Split, Croatia*

Accepted 2016 October 4. Received 2016 October 3; in original form 2016 June 17; Editorial Decision 2016 October 3

ABSTRACT

We reduced European Southern Observatory’s archival linear spectropolarimetry data (4000–9000 Å) of six highly polarized and eight unpolarized standard stars observed between 2010 and 2016, for a total of 70 epochs, with the Focal Reducer and low dispersion Spectrograph (FORS2) mounted at the Very Large Telescope. We provide very accurate standard stars polarization measurements as a function of wavelength, and test the performance of the spectropolarimetric mode (PMOS) of FORS2. We used the unpolarized stars to test the time stability of the PMOS mode, and found a small (≤ 0.1 per cent), but statistically significant, on-axis instrumental polarization wavelength dependence, possibly caused by the tilted surfaces of the dispersive element. The polarization degree and angle are found to be stable at the level of ≤ 0.1 per cent and ≤ 0.2 degrees, respectively. We derived the polarization wavelength dependence of the polarized standard stars and found that, in general, the results are consistent with those reported in the literature, e.g. Fossati et al., who performed a similar analysis using FORS1 data. The re-calibrated data provide a very accurate set of standards, which can be very reliably used for technical and scientific purposes. The analysis of the Serkowski parameters revealed a systematic deviation from the width parameter K reported by Whittet et al. This is

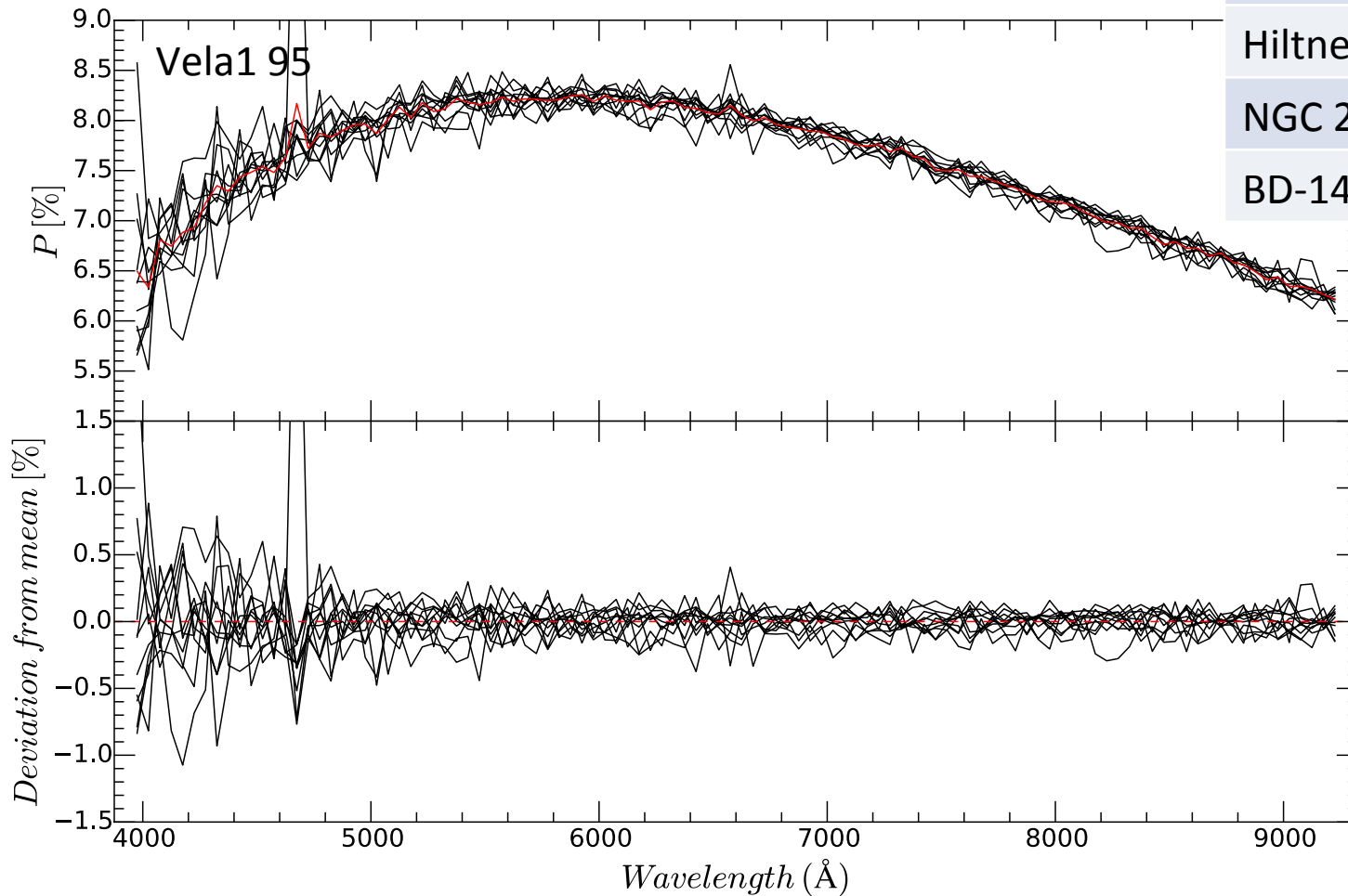
Results: unpolarized stars

Fossati et al. 2007

- analysis with FORS1 data from 1999 – 2005
 - PMOS: $P_U \sim 0.0\%$
 $P_Q(B) = 0.07 \pm 0.01 \%$
 $P_Q(V) = 0.09 \pm 0.01 \%$
 - IPOL: $P_U \sim 0.0\%$, $P_Q \sim 0.0\%$
- Their conclusion: PMOS offset might be associated with some, but not all, grism and filter combinations.
-
- Source of polarization unclear, but likely related to tilted surfaces of the dispersive element.

Results: polarized stars

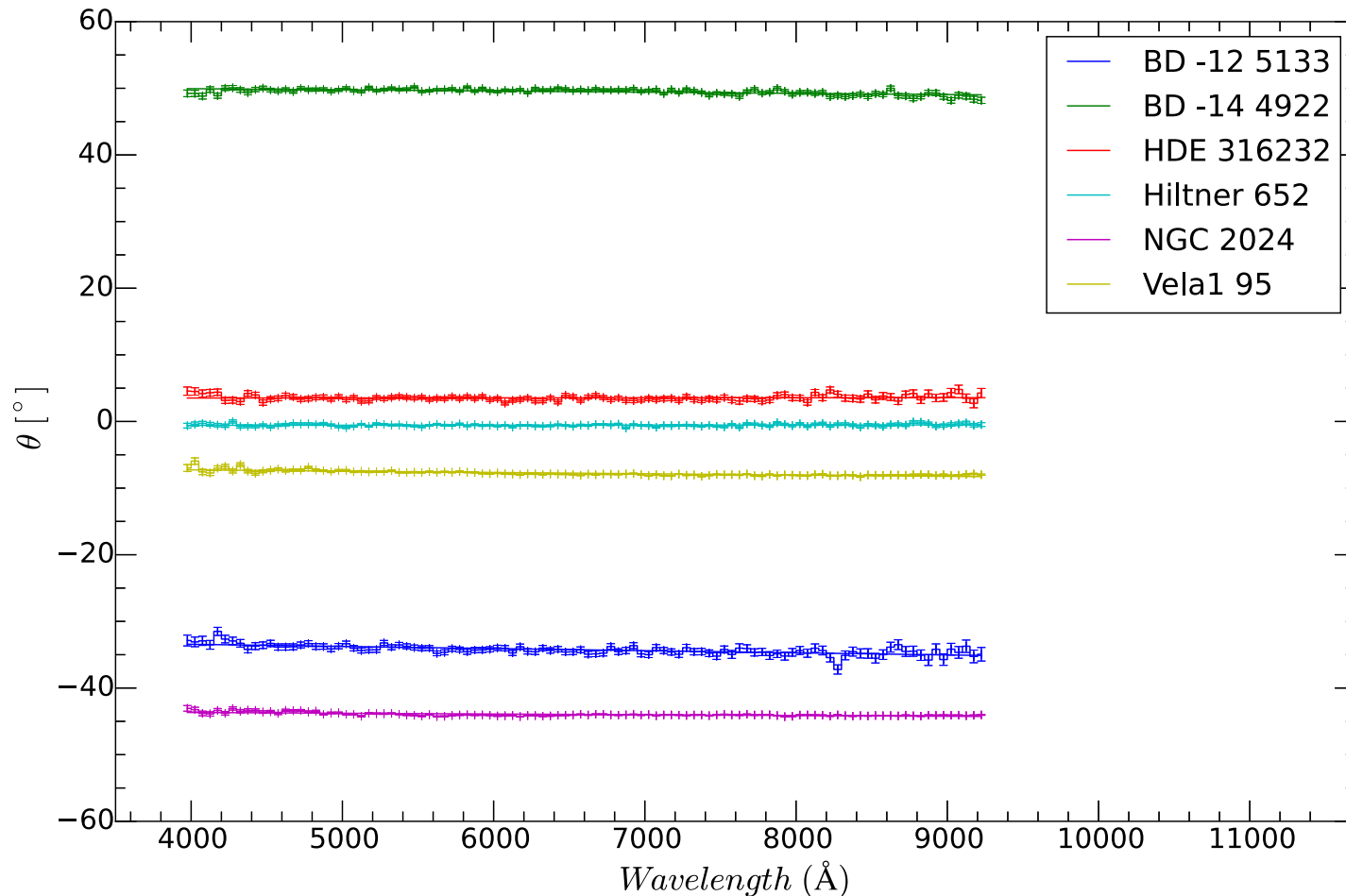
Reproducibility of polarization



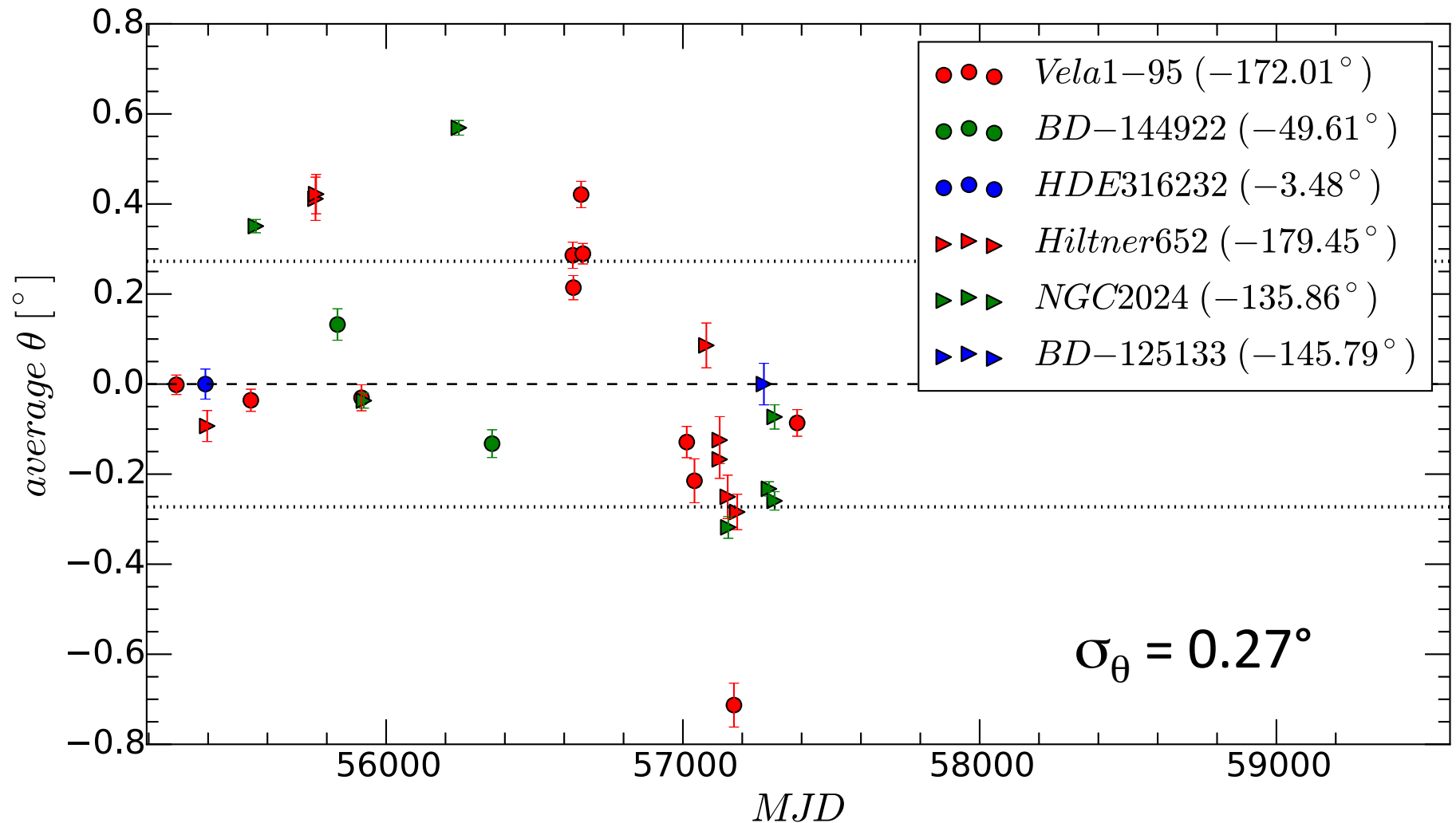
Name	#	rms
Vela1 95	11	0.21%
Hiltner 625	8	0.12%
NGC 2424 1	7	0.12%
BD-144922	2	0.05%

Results: polarization angle

- No significant θ - λ dependence
- Slopes $d\theta/d\lambda$ between -2.5 and 0.53 degree μm^{-1}



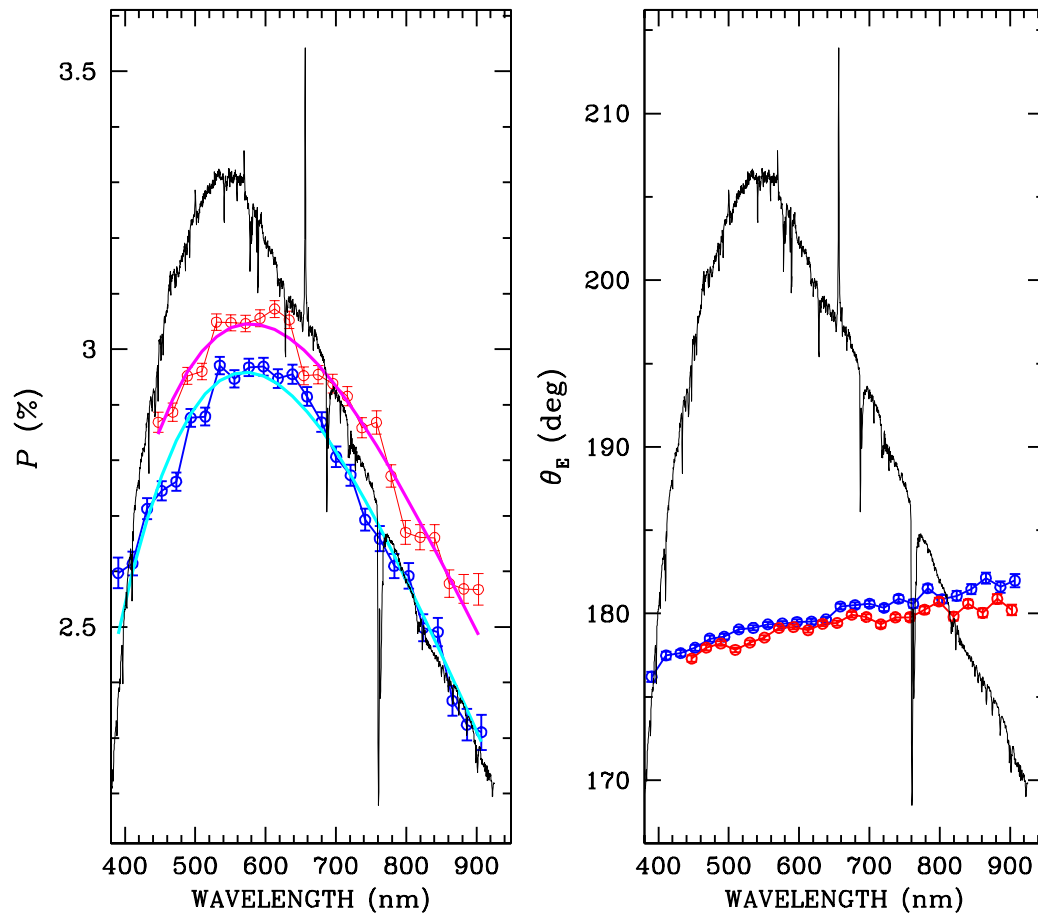
Results: polarization angle



Polarization degree inconsistencies

Bagnulo et al., in preparation

HD149404 2015-05-12

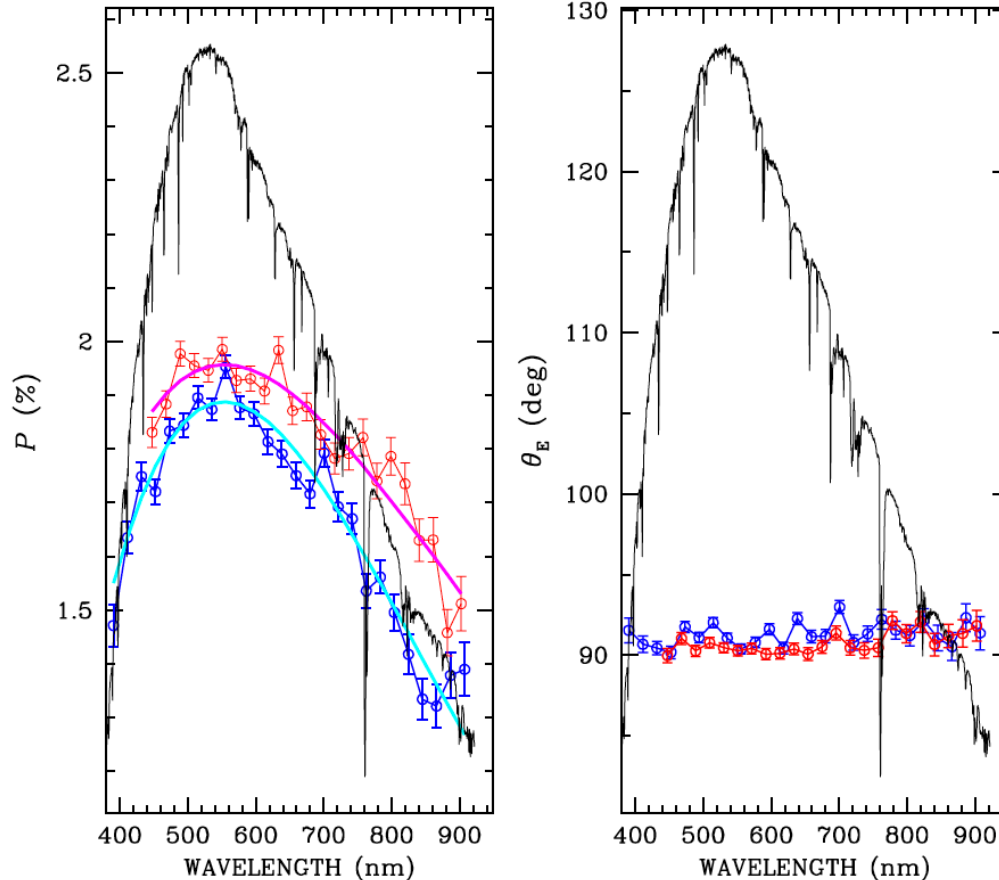


- The Large Instellar Polarization Survey (LIPS)
- Program ID: 095.C-0855, 096.C-0159; PI: Cox, N.
- ~104 stars observed with VLT/ FORS2 in spectropolarimetric mode
- 22 stars have been observed twice.
- In about 10% of the LIPS observations we observe an inconsistency between polarization measurements

Polarization degree inconsistencies

Bagnulo et al., in preparation

HD108639 2016-01-23



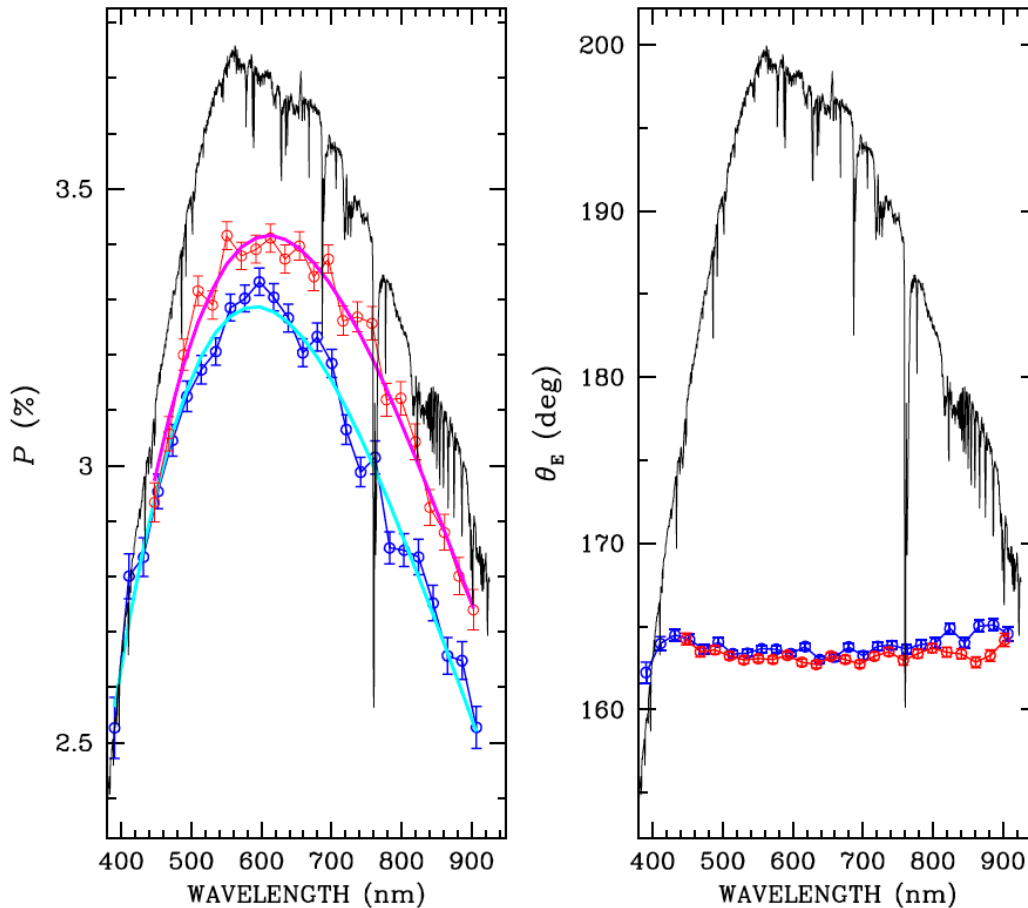
- The Large Instellar Polarization Survey (LIPS)
- Program ID: 095.C-0855, 096.C-0159; PI: Cox, N.
- ~104 stars observed with VLT/ FORS2 in spectropolarimetric mode
- 22 stars have been observed twice.
- In about 10% of the LIPS observations we observe an inconsistency between polarization measurements

Polarization degree inconsistencies

Bagnulo et al., in preparation

HD80558

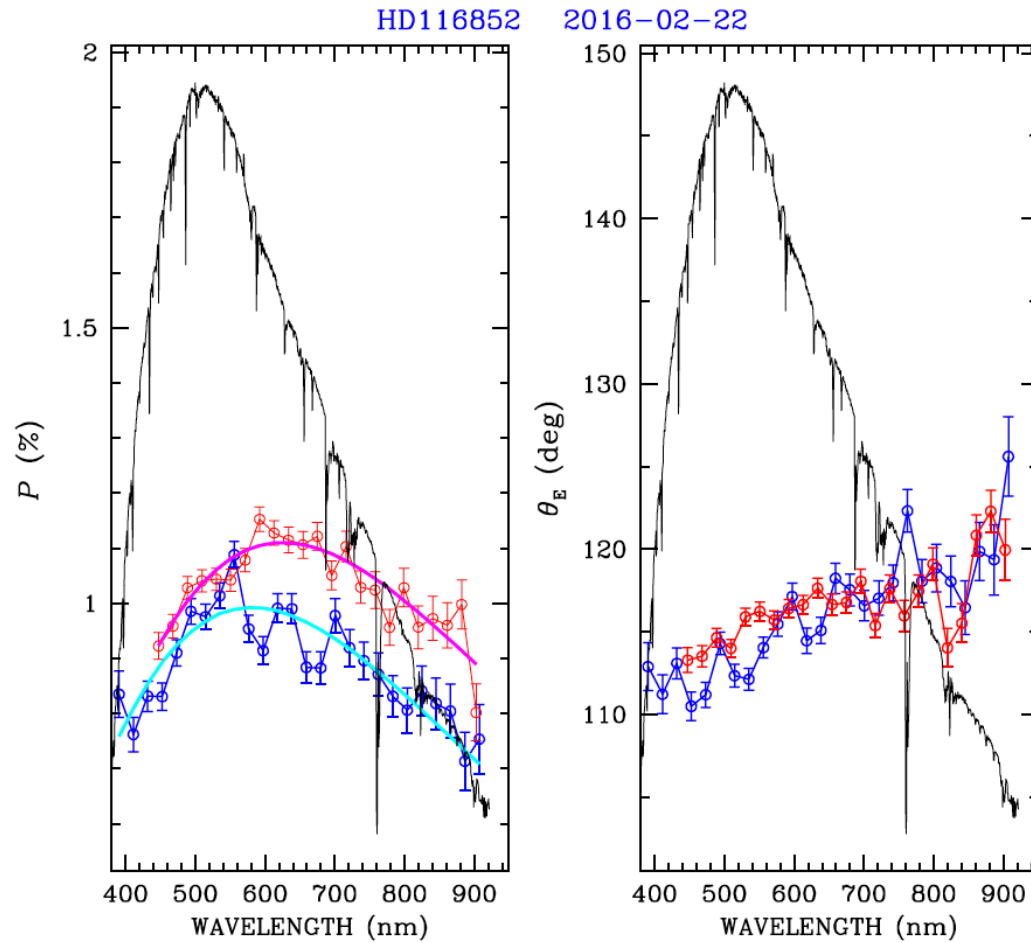
2015-05-23



- The Large Instellar Polarization Survey (LIPS)
- Program ID: 095.C-0855, 096.C-0159; PI: Cox, N.
- ~104 stars observed with VLT/ FORS2 in spectropolarimetric mode
- 22 stars have been observed twice.
- In about 10% of the LIPS observations we observe an inconsistency between polarization measurements

Polarization degree inconsistencies

Bagnulo et al., in preparation

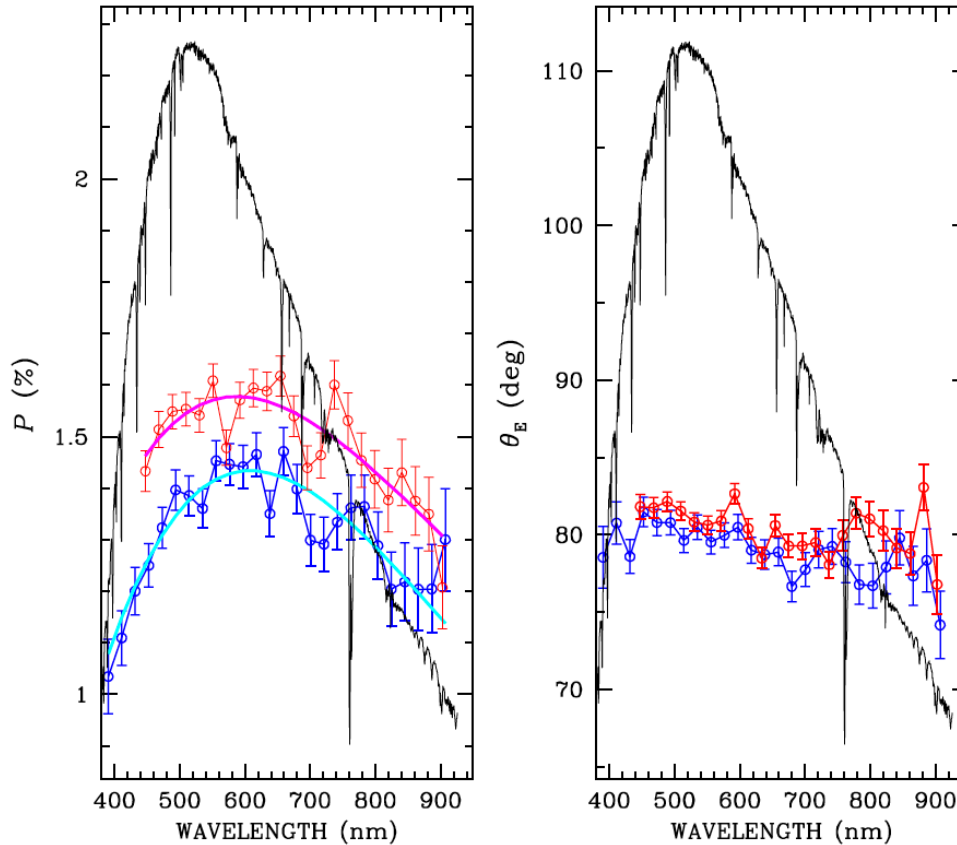


- The Large Instellar Polarization Survey (LIPS)
- Program ID: 095.C-0855, 096.C-0159; PI: Cox, N.
- ~104 stars observed with VLT/ FORS2 in spectropolarimetric mode
- 22 stars have been observed twice.
- In about 10% of the LIPS observations we observe an inconsistency between polarization measurements

Polarization degree inconsistencies

Bagnulo et al., in preparation

HD129557 2015-05-11



- The Large Instellar Polarization Survey (LIPS)
- Program ID: 095.C-0855, 096.C-0159; PI: Cox, N.
- ~104 stars observed with VLT/ FORS2 in spectropolarimetric mode
- 22 stars have been observed twice.
- In about 10% of the LIPS observations we observe an inconsistency between polarization measurements

Effect of HWP positioning inaccuracy

$$S(\alpha, \beta, \gamma) \propto \frac{1}{2} \{ I + [Q \cos 2\alpha + U \sin 2\alpha] \cos(2\beta - 2\alpha) \\ - [Q \sin 2\alpha - U \cos 2\alpha] \sin(2\beta - 2\alpha) \cos \gamma \\ + V \sin(2\beta - 2\alpha) \sin \gamma \}.$$

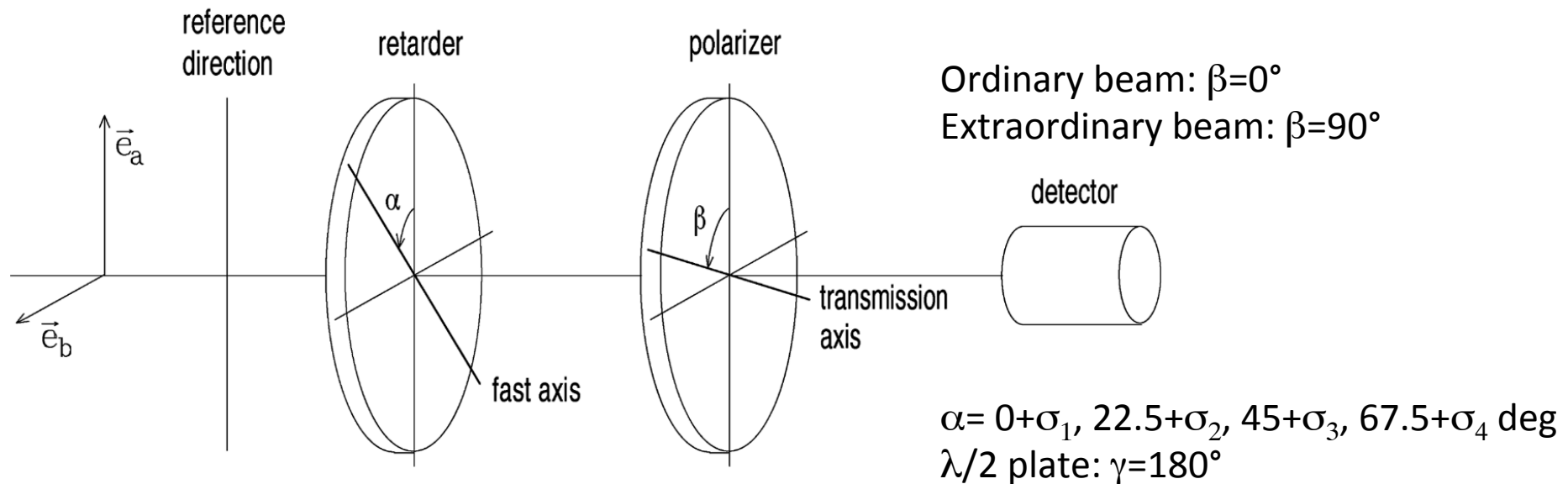
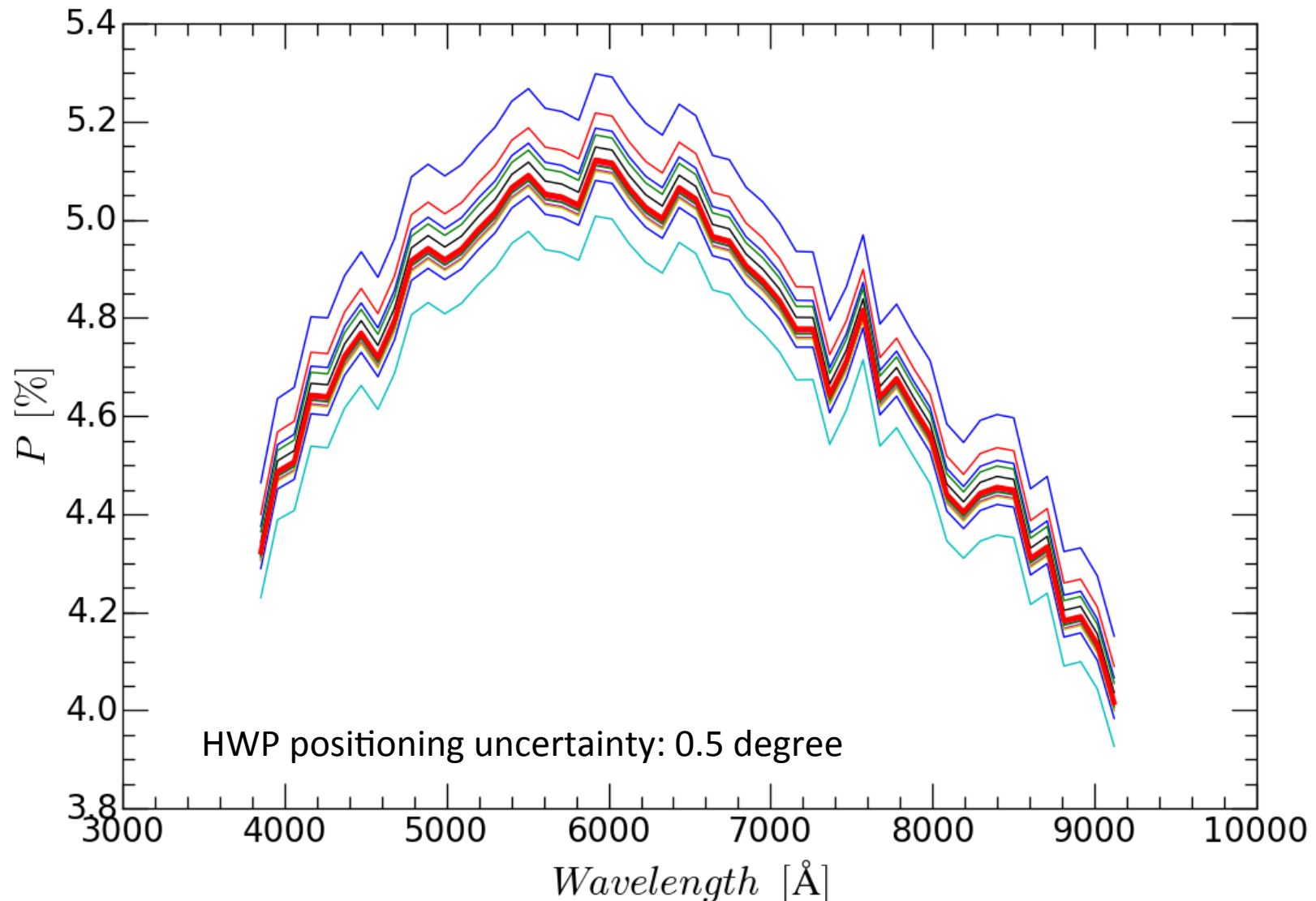


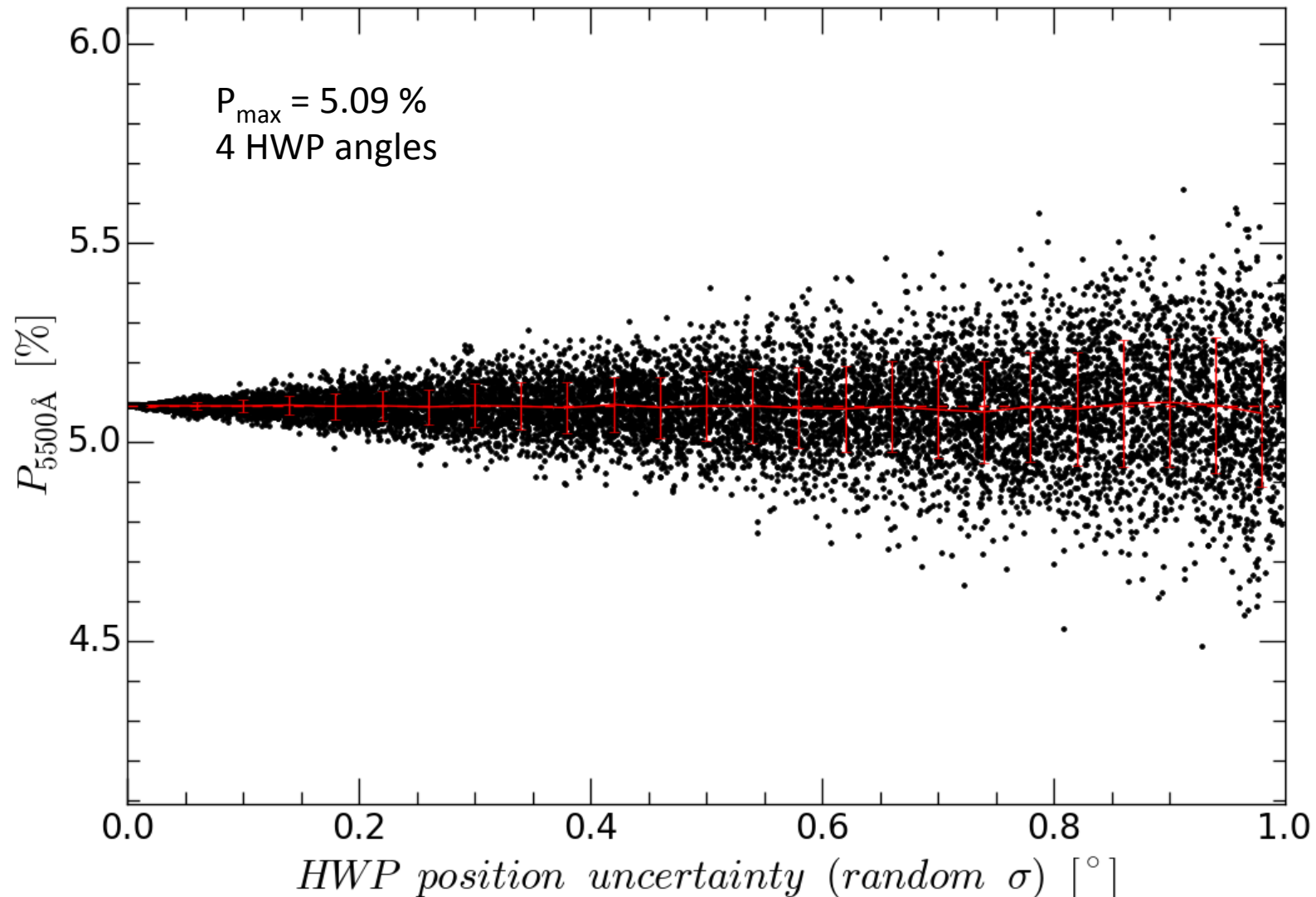
FIG. 1.—Schematic representation of an ideal polarimeter (from Landi Degl’Innocenti & Landolfi 2004).

Bagnulo et al. 2009

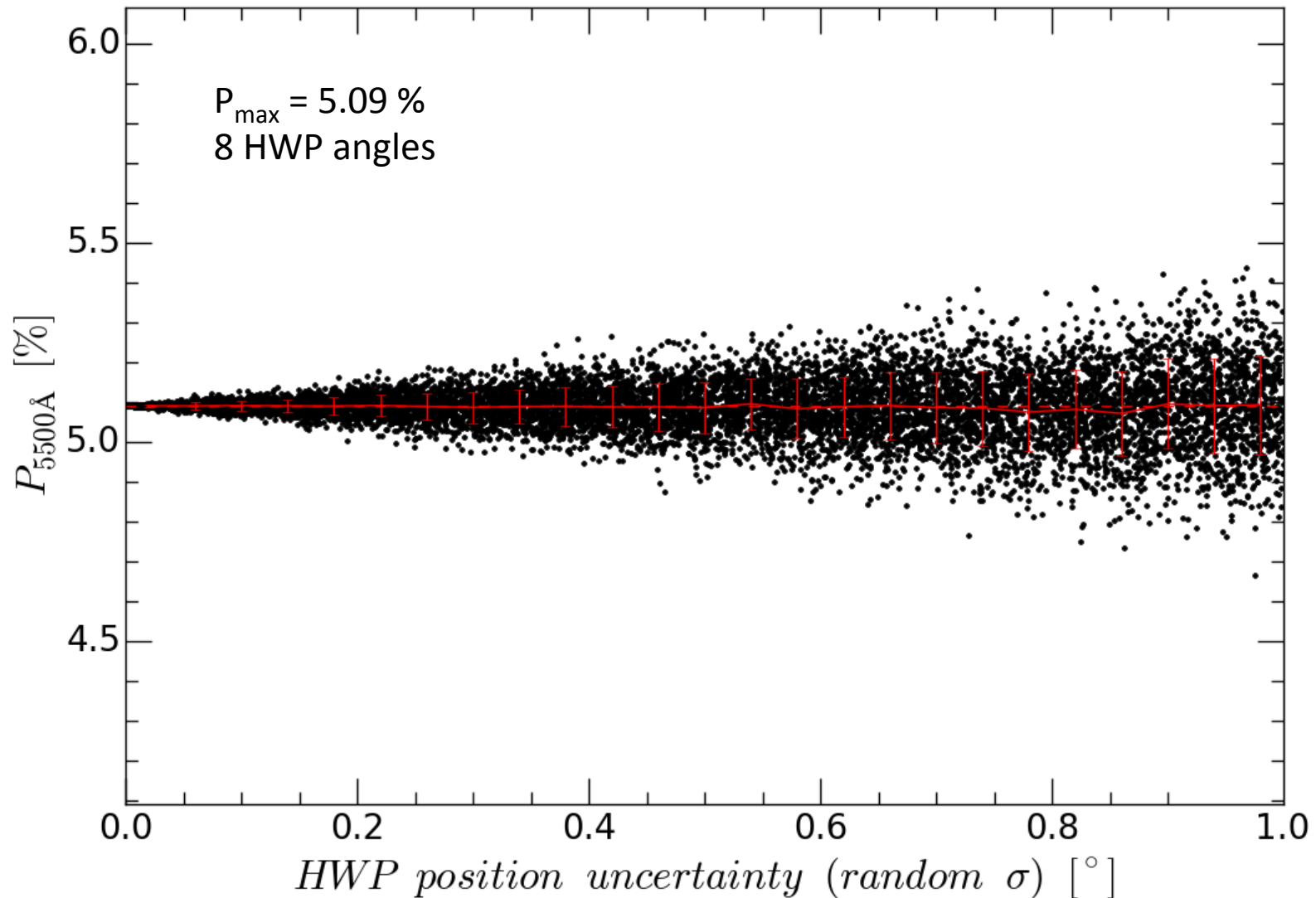
Effect of HWP positioning inaccuracy



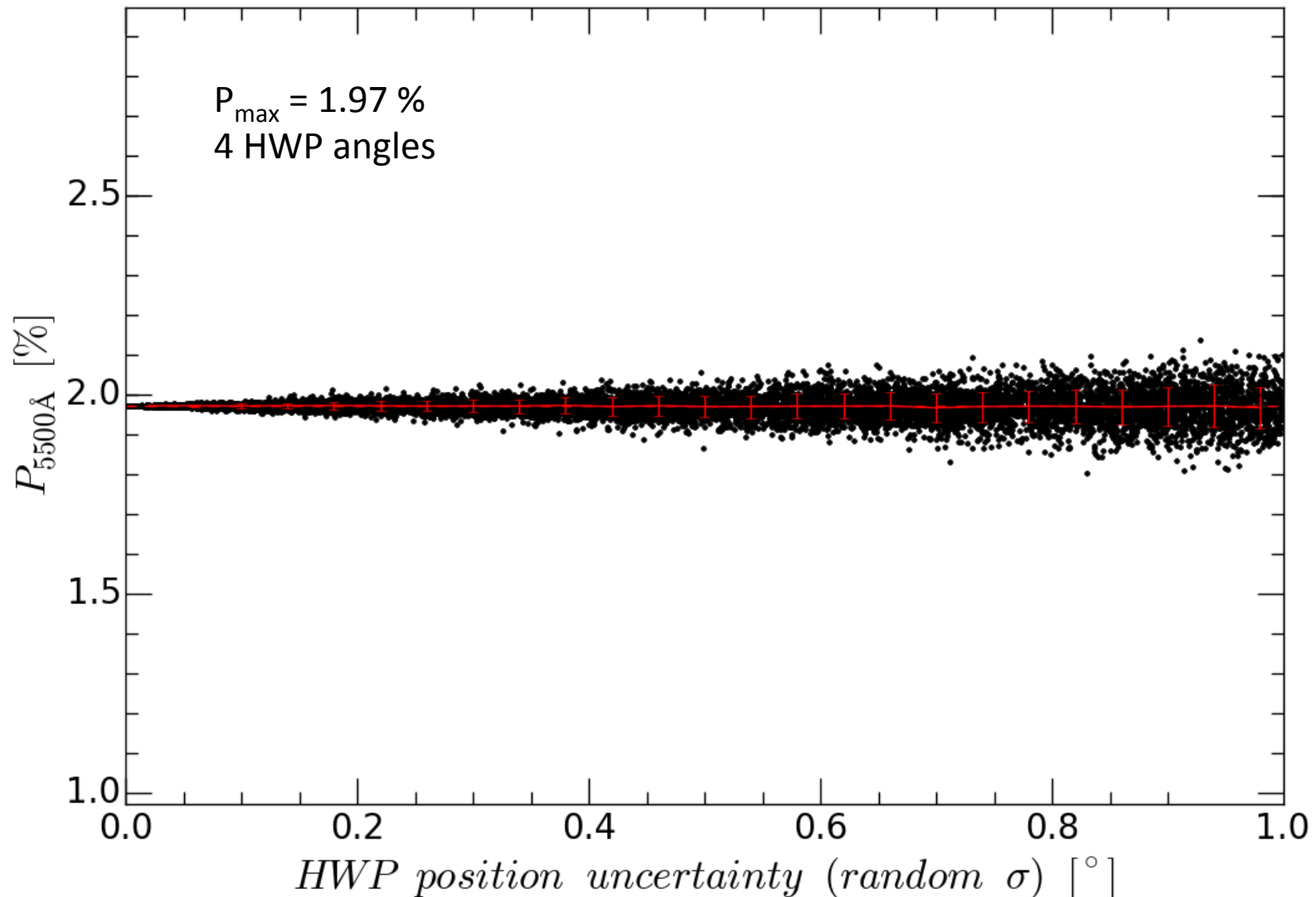
Effect of HWP positioning inaccuracy



Effect of HWP positioning inaccuracy



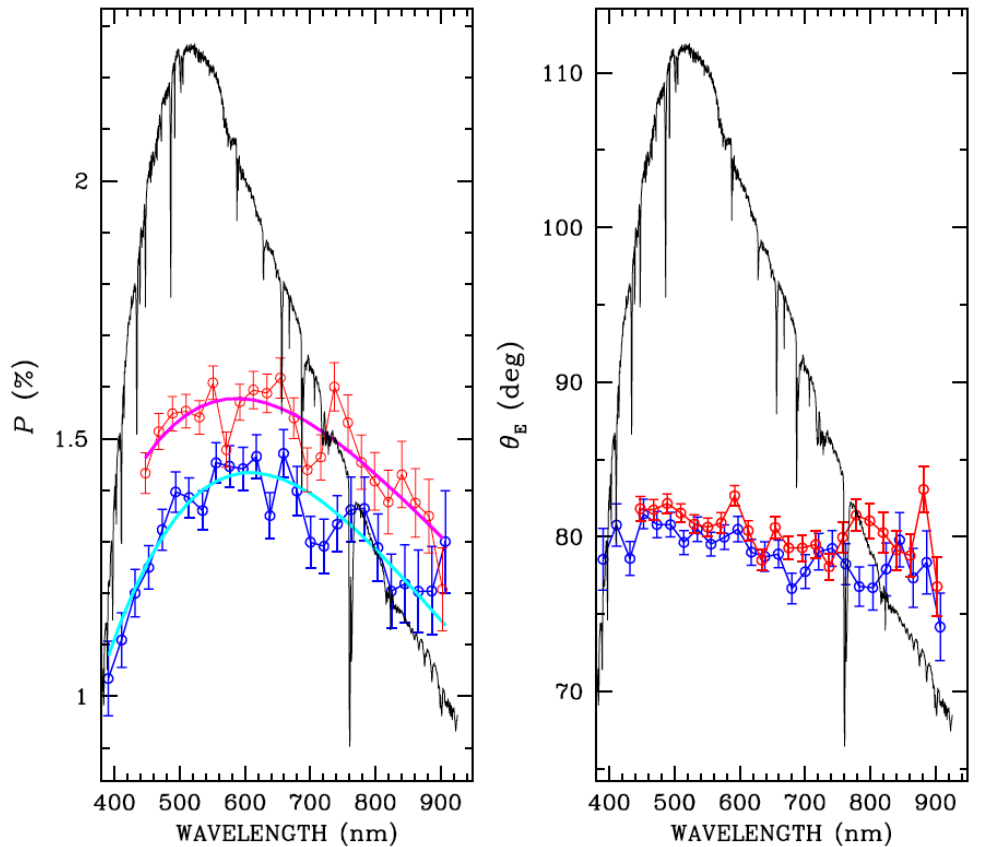
Effect of HWP positioning inaccuracy



Effect of slit on polarization

Bagnulo et al., in preparation

HD129557 2015-05-11



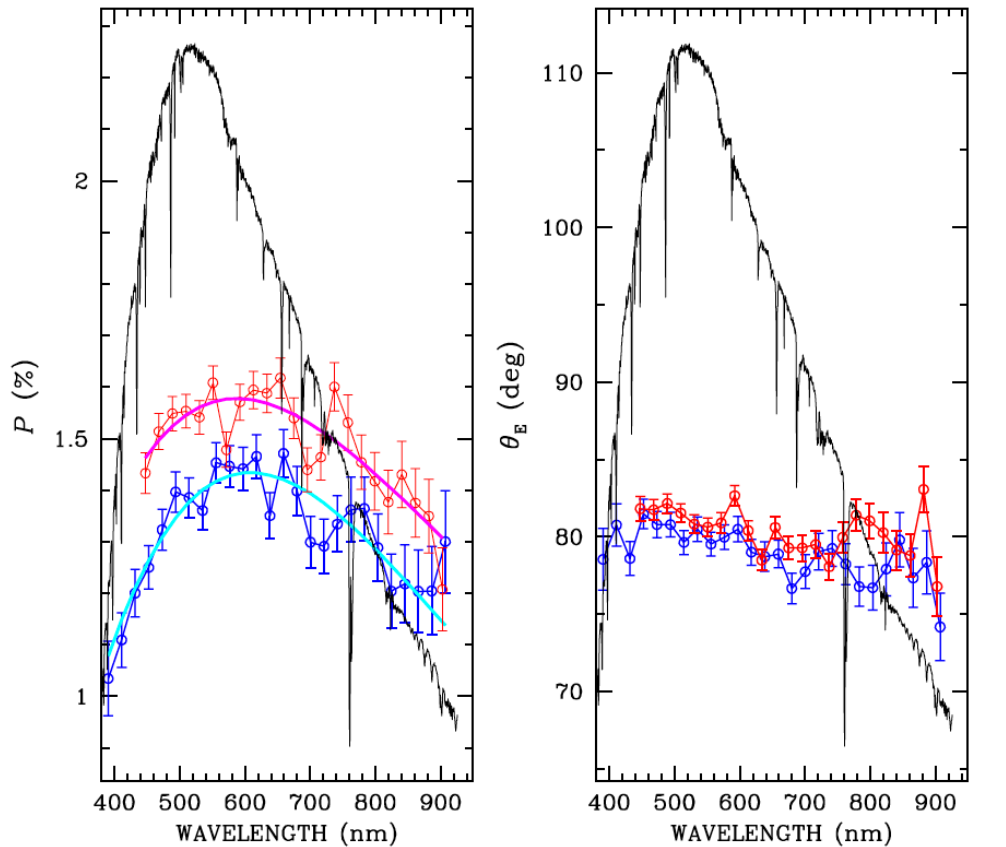
Hypothesis: due to atmospheric disturbances (seeing), the star reaches the edge of the slit, which causes diffraction of the light, and additional polarization (Keller+ 2002).



Effect of slit on polarization

Bagnulo et al., in preparation

HD129557 2015-05-11



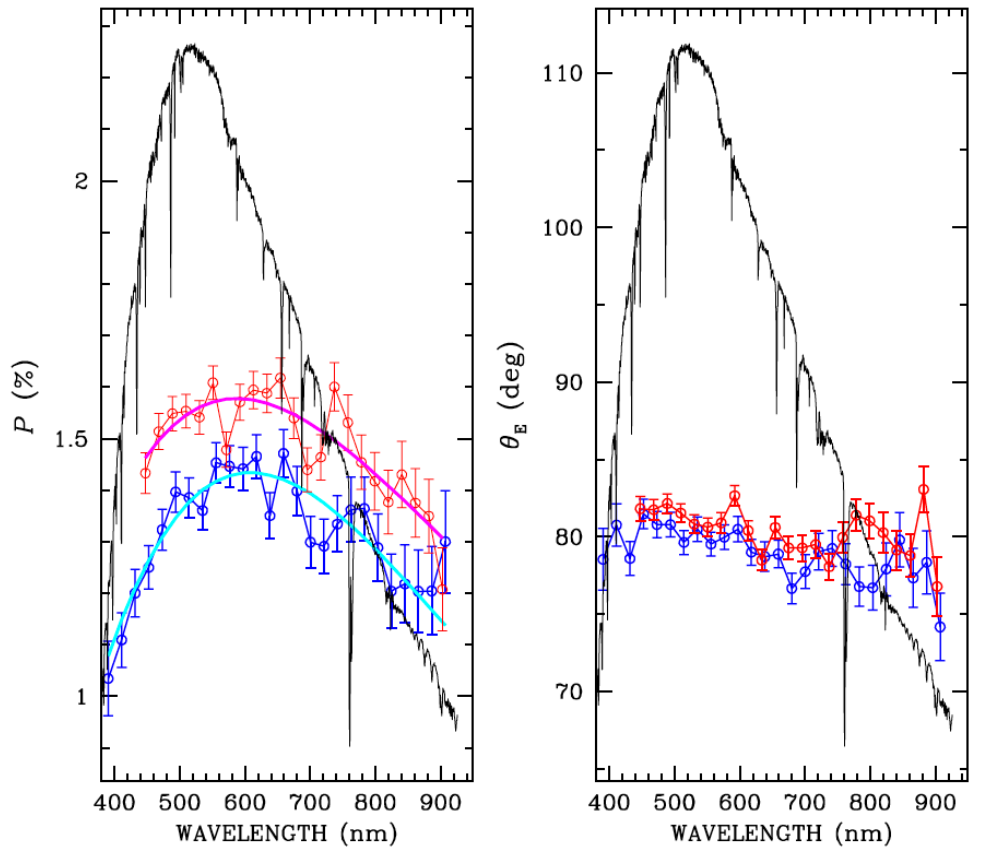
Hypothesis: due to atmospheric disturbances (seeing), the star reaches the edge of the slit, which causes diffraction of the light, and additional polarization (Keller+ 2002).



Effect of slit on polarization

Bagnulo et al., in preparation

HD129557 2015-05-11



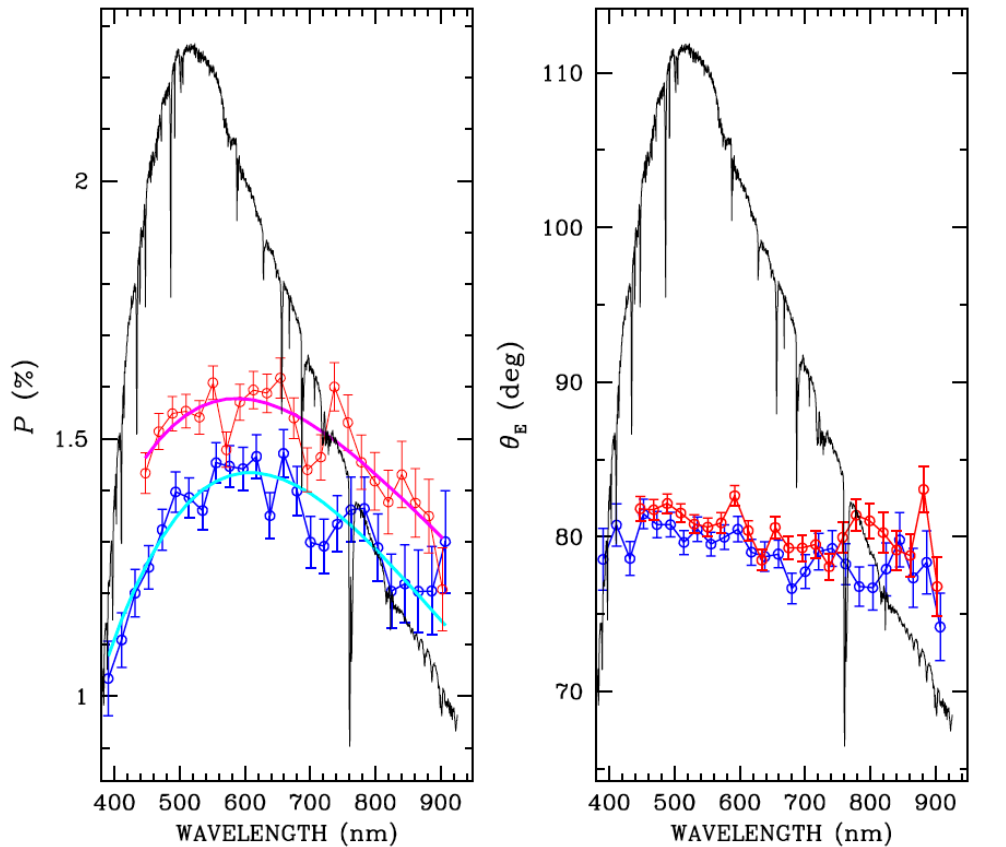
Hypothesis: due to atmospheric disturbances (seeing), the star reaches the edge of the slit, which causes diffraction of the light, and additional polarization (Keller+ 2002).



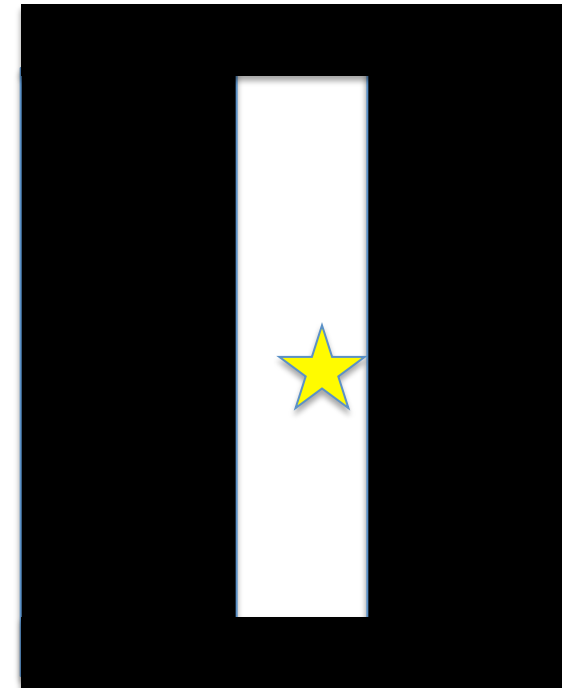
Effect of slit on polarization

Bagnulo et al., in preparation

HD129557 2015-05-11



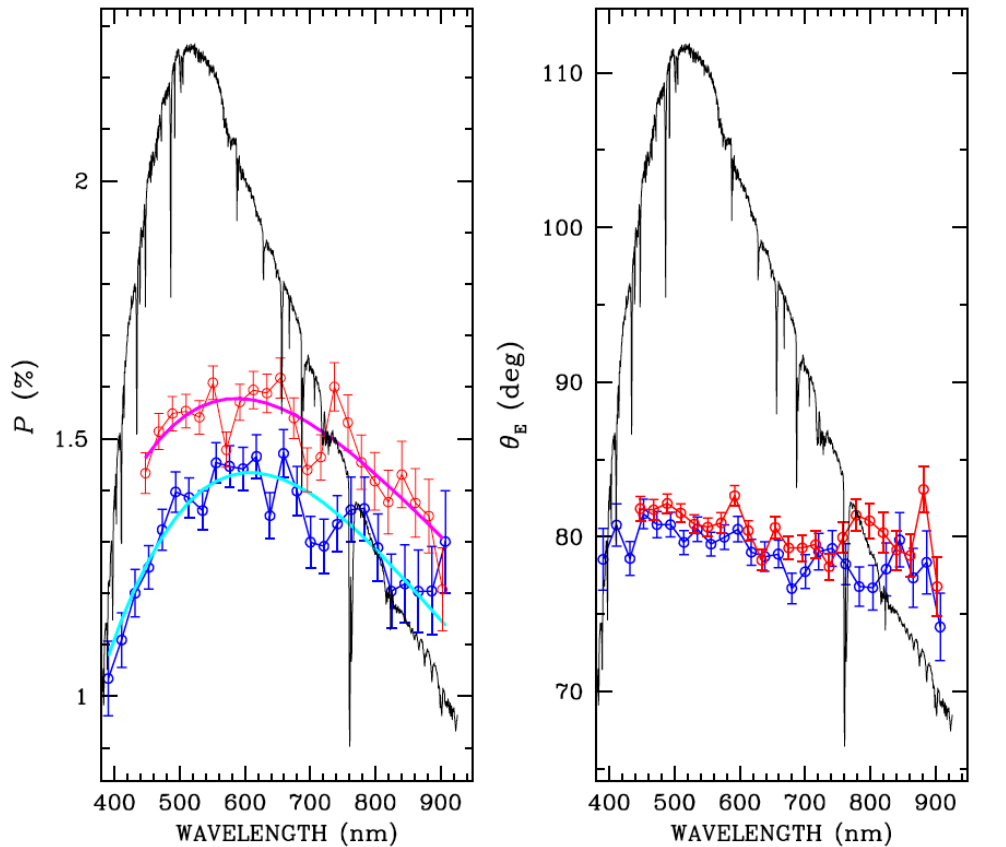
Hypothesis: due to atmospheric disturbances (seeing), the star reaches the edge of the slit, which causes diffraction of the light, and additional polarization (Keller+ 2002).



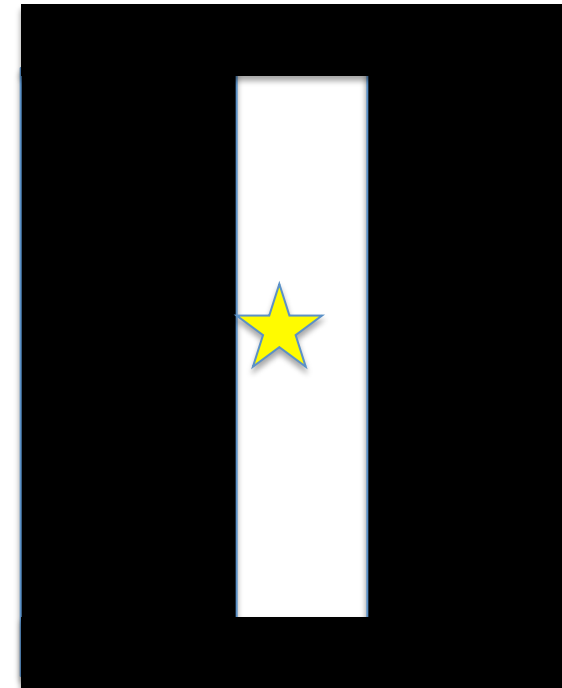
Effect of slit on polarization

Bagnulo et al., in preparation

HD129557 2015-05-11



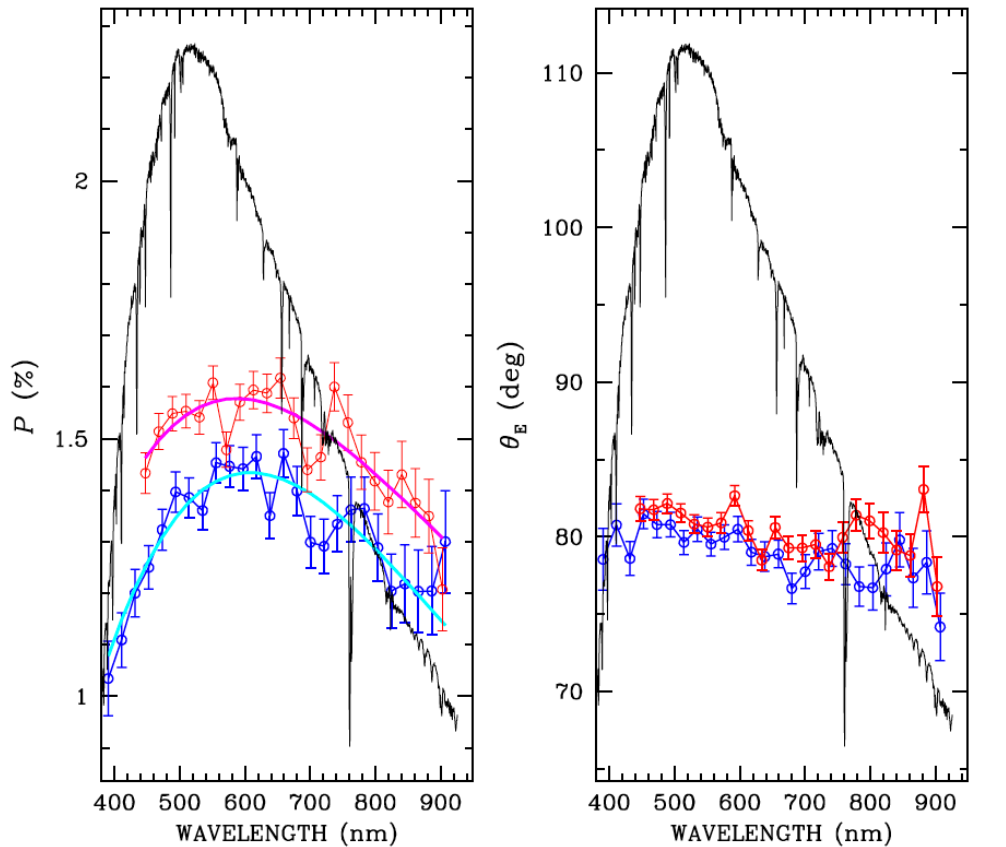
Hypothesis: due to atmospheric disturbances (seeing), the star reaches the edge of the slit, which causes diffraction of the light, and additional polarization (Keller+ 2002).



Effect of slit on polarization

Bagnulo et al., in preparation

HD129557 2015-05-11



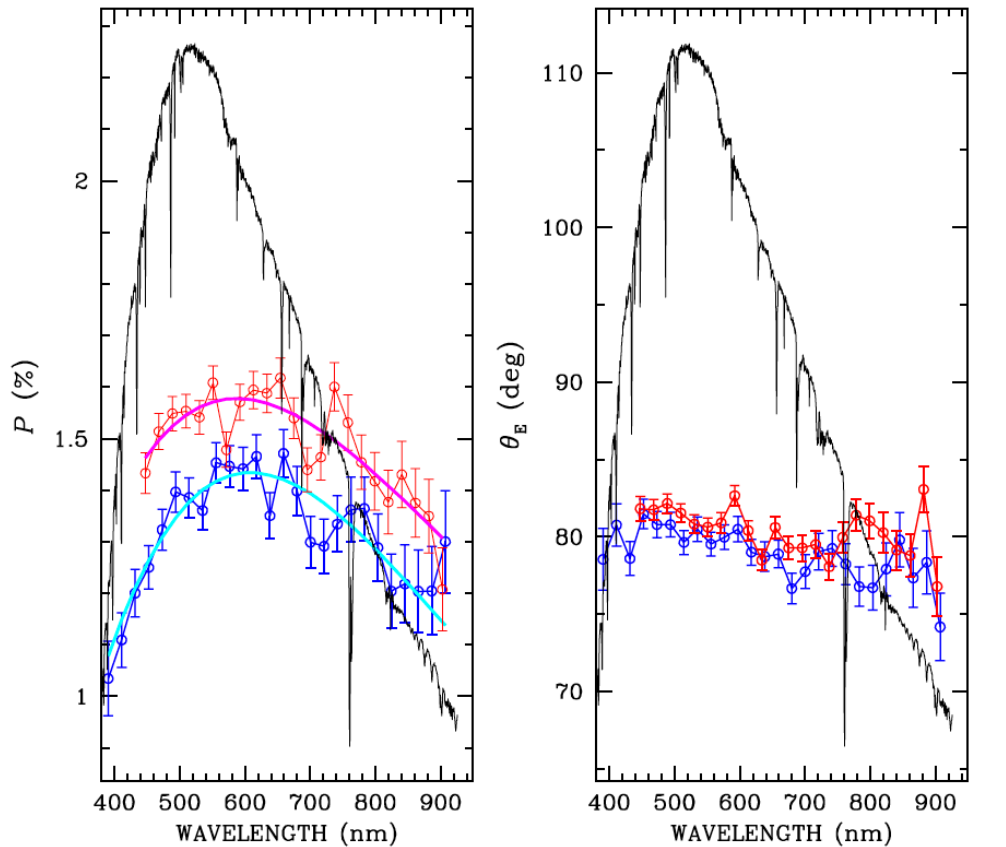
Hypothesis: due to atmospheric disturbances (seeing), the star reaches the edge of the slit, which causes diffraction of the light, and additional polarization (Keller+ 2002).



Effect of slit on polarization

Bagnulo et al., in preparation

HD129557 2015-05-11



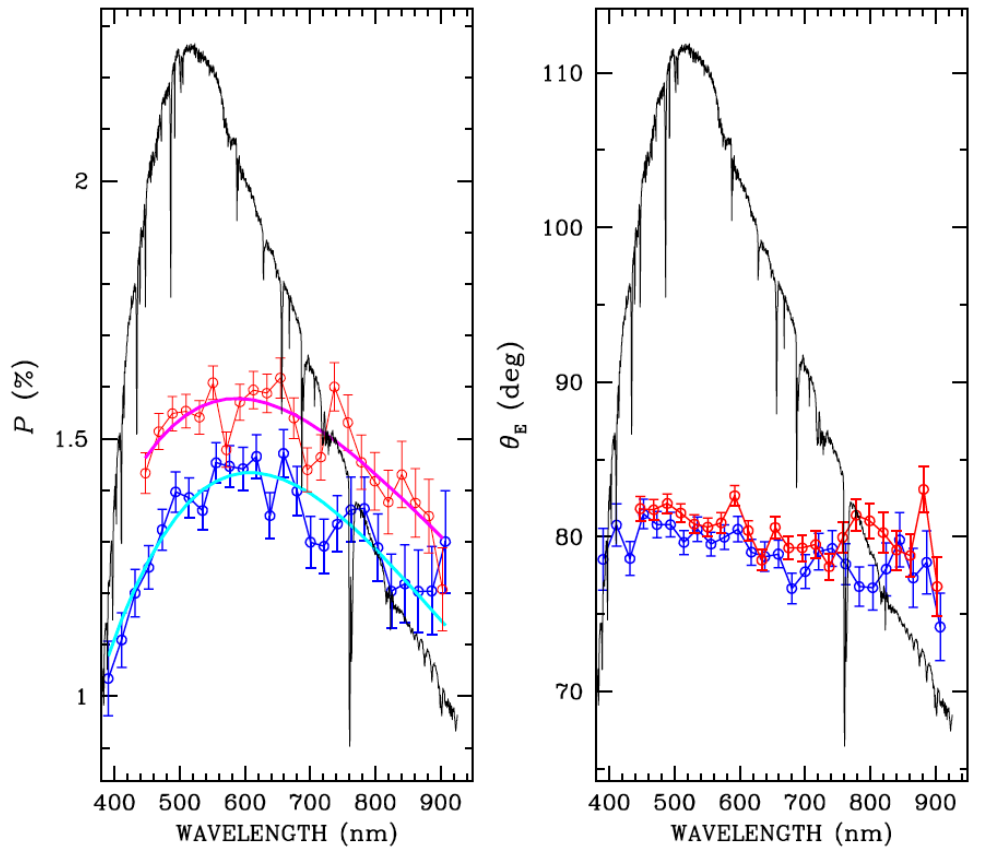
Hypothesis: due to atmospheric disturbances (seeing), the star reaches the edge of the slit, which causes diffraction of the light, and additional polarization (Keller+ 2002).



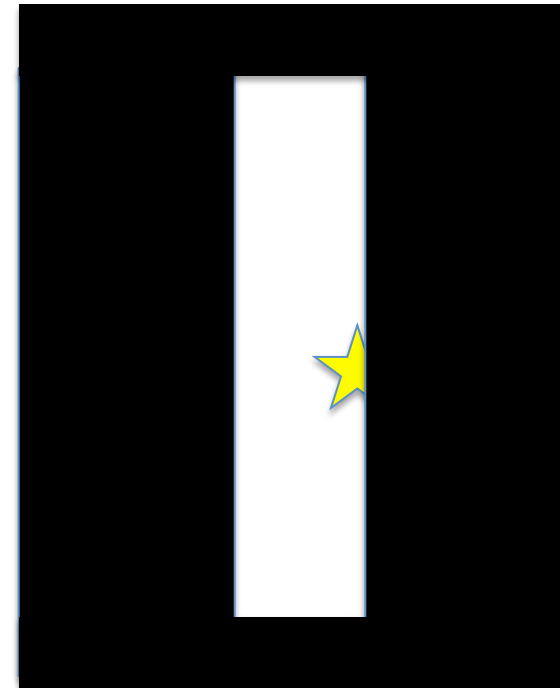
Effect of slit on polarization

Bagnulo et al., in preparation

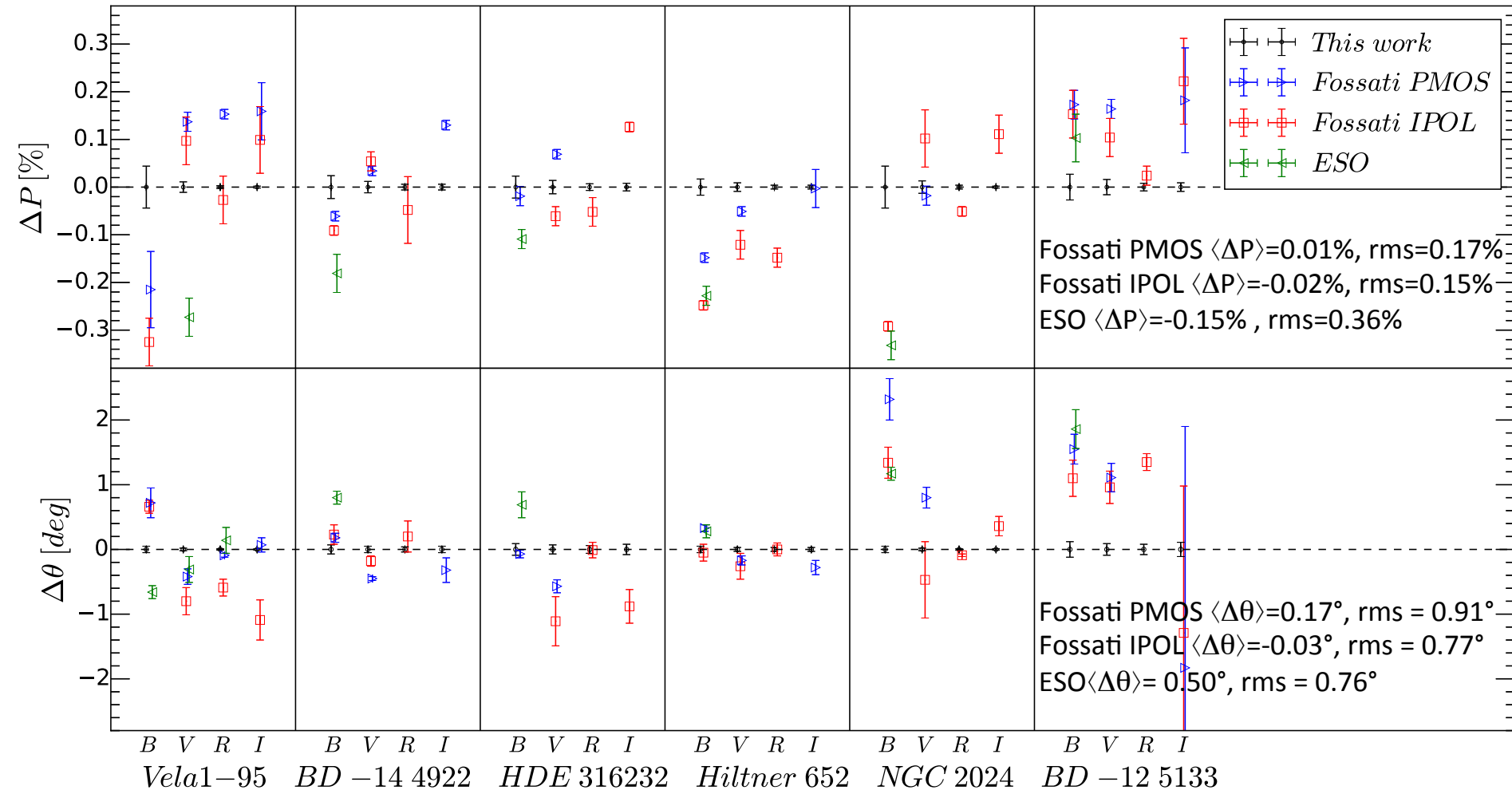
HD129557 2015-05-11



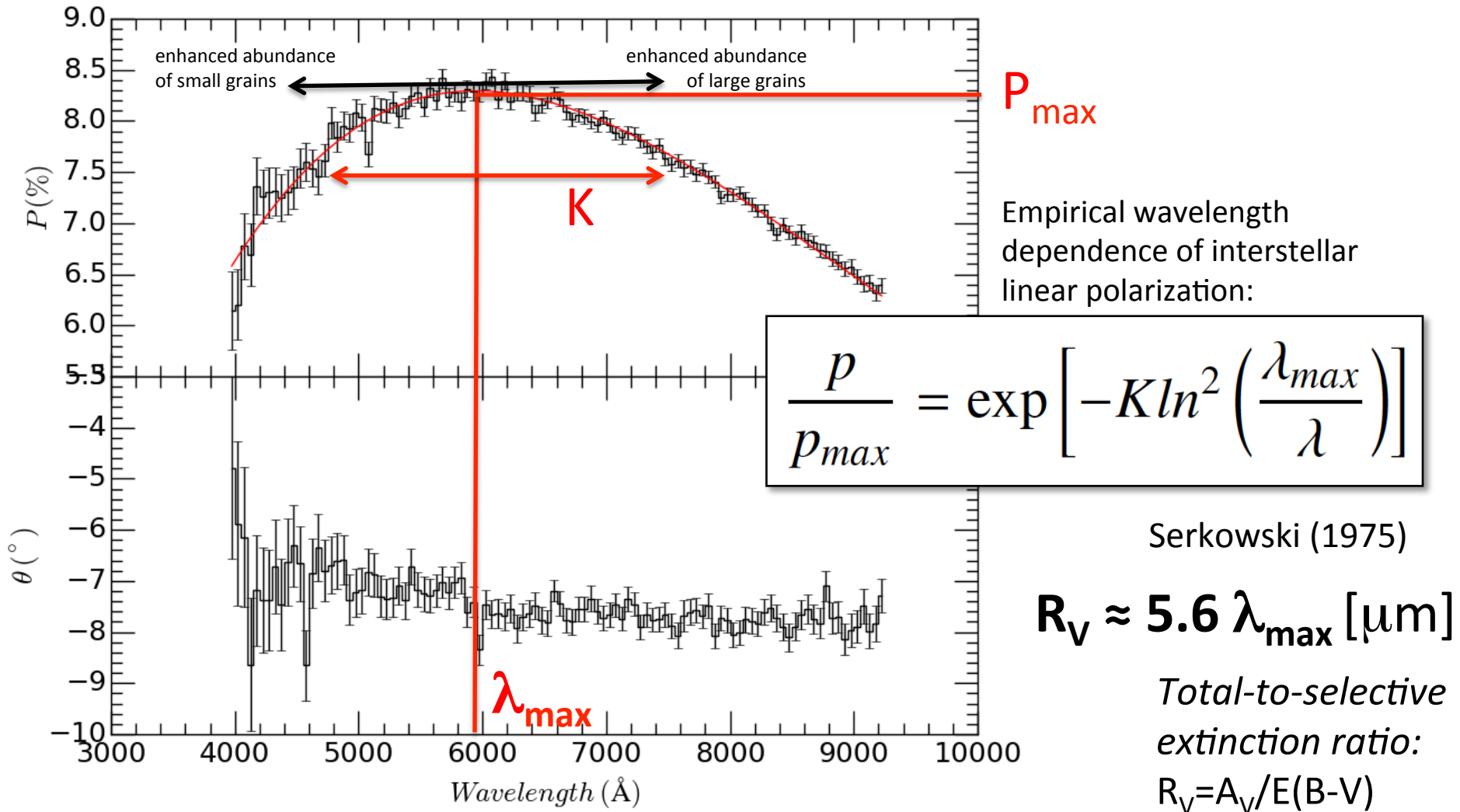
Hypothesis: due to atmospheric disturbances (seeing), the star reaches the edge of the slit, which causes diffraction of the light, and additional polarization (Keller+ 2002).

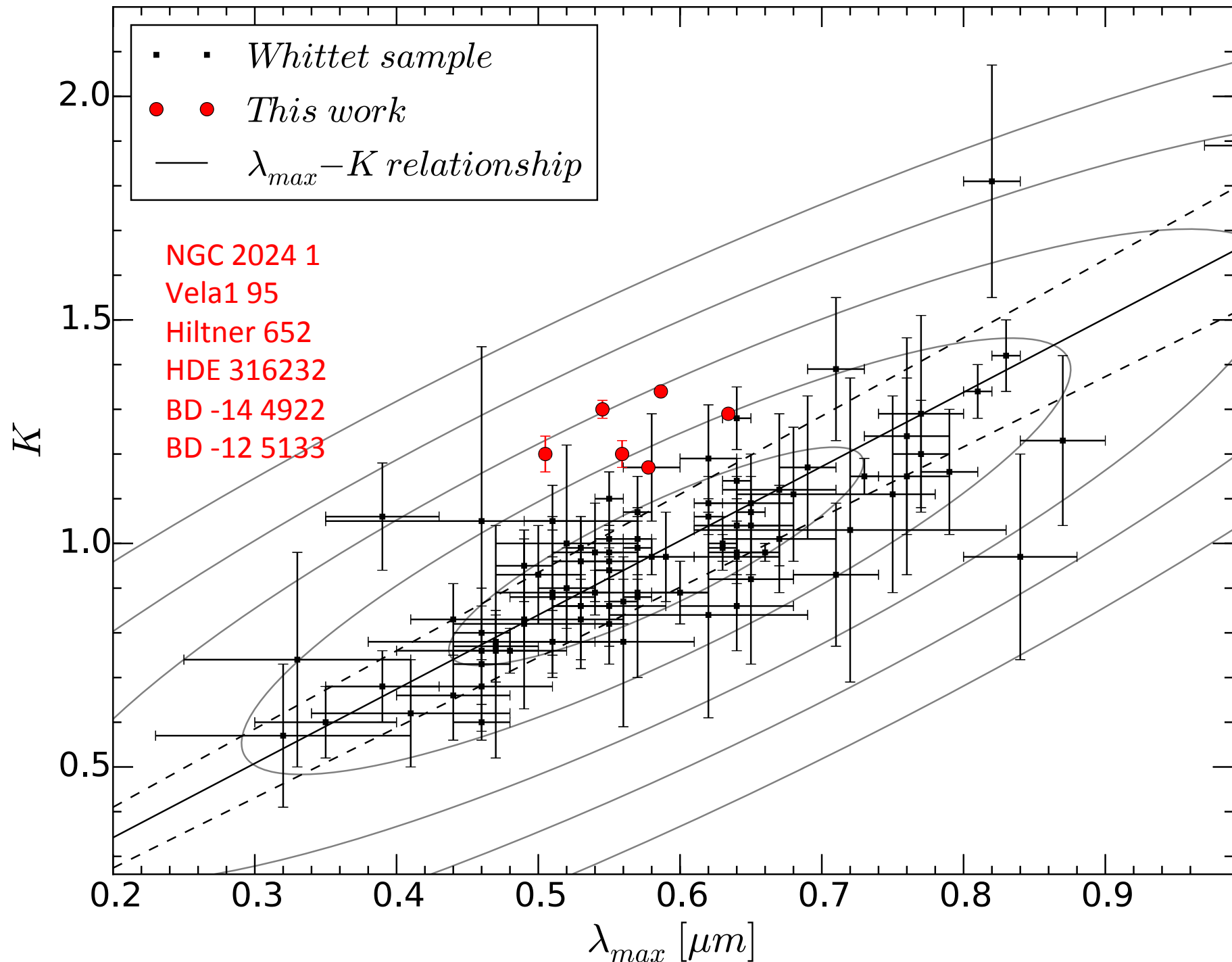


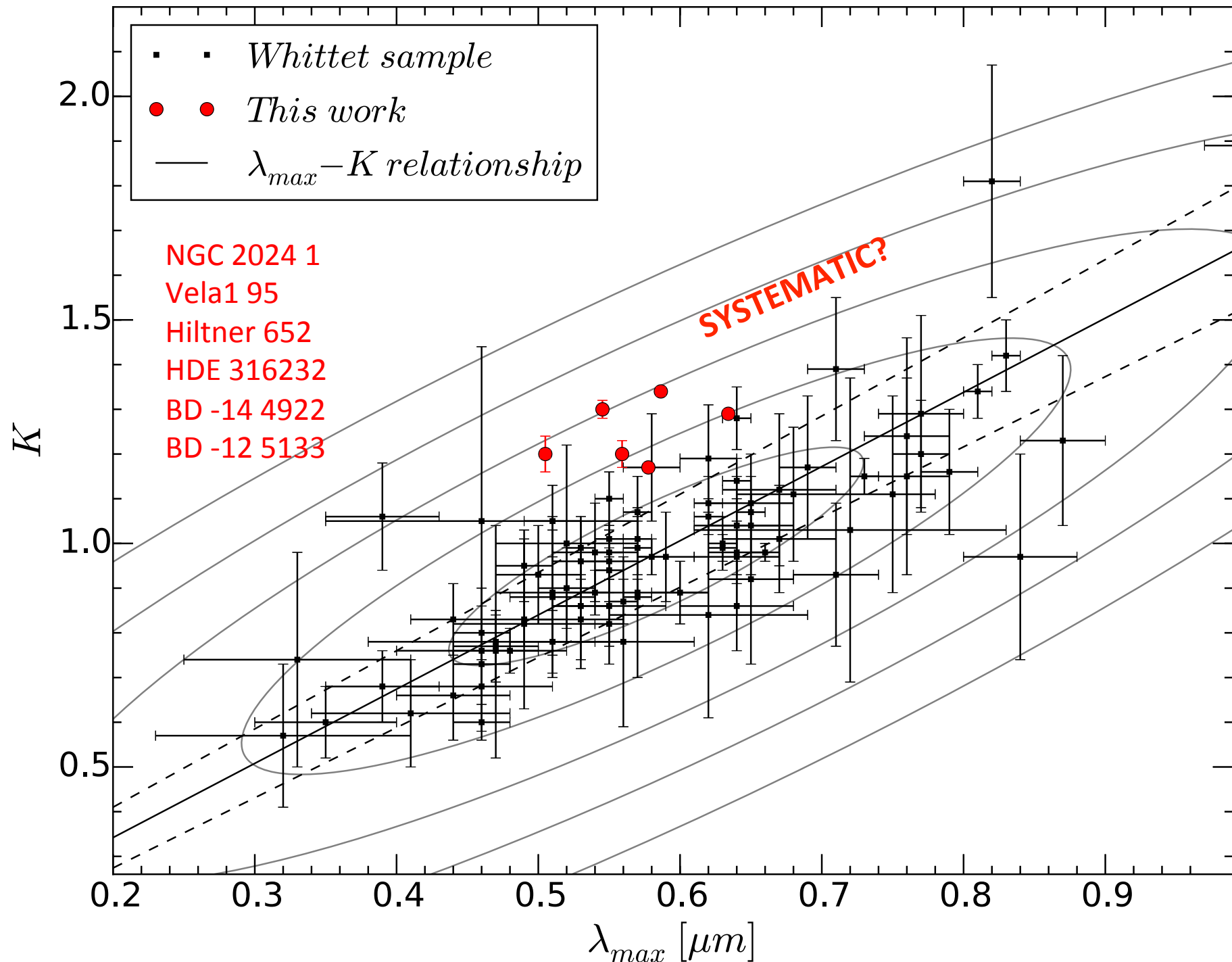
Comparison with literature

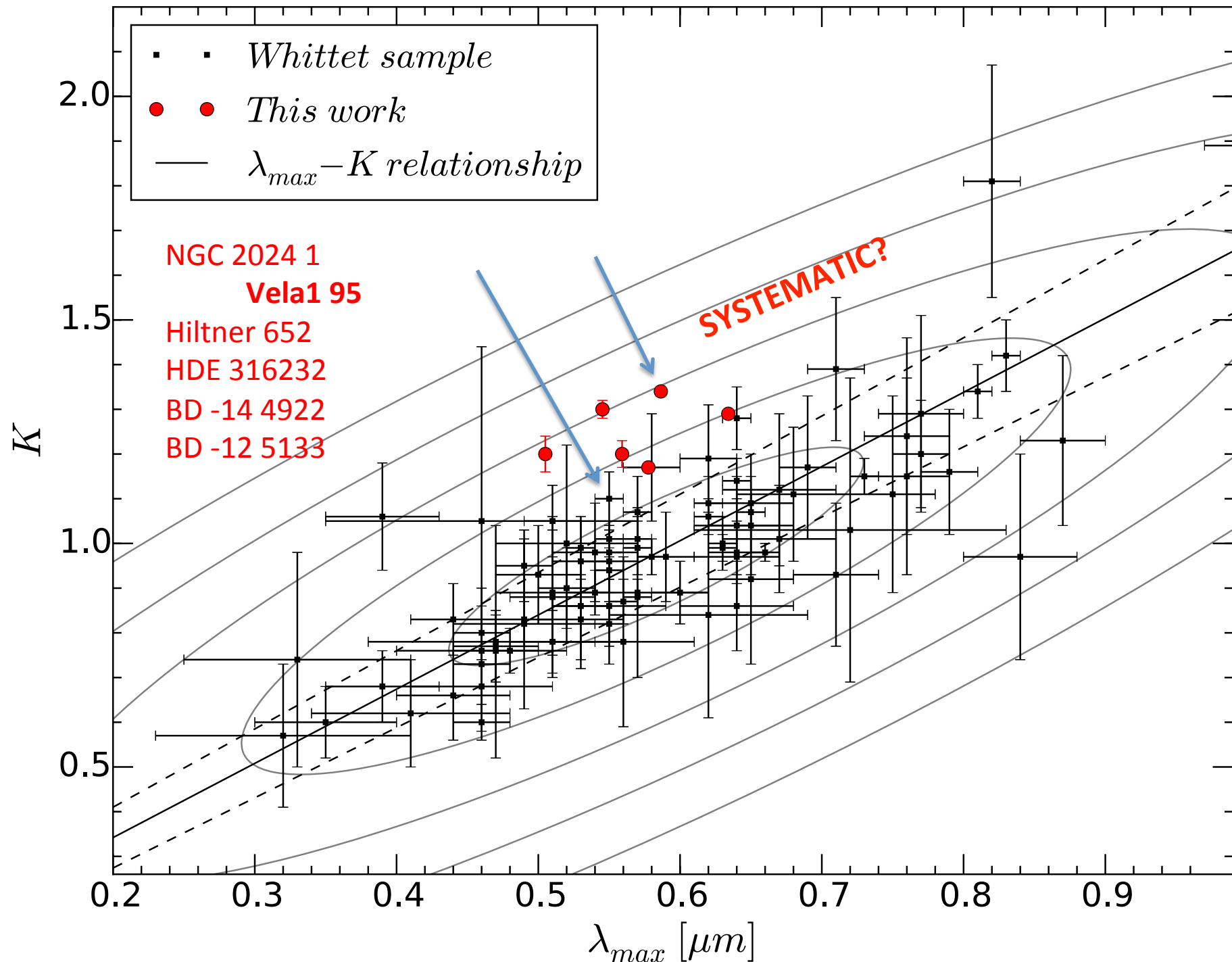


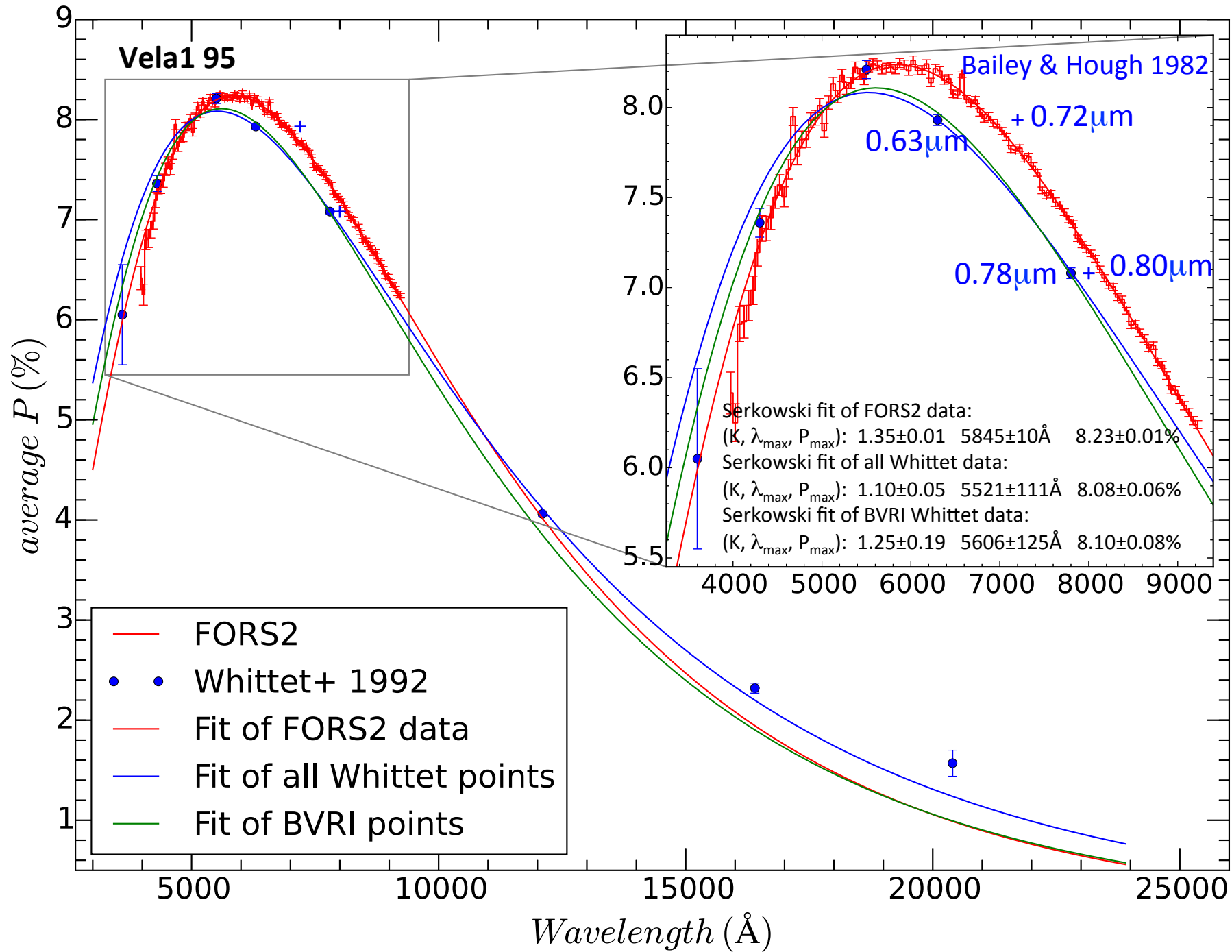
Serkowski law



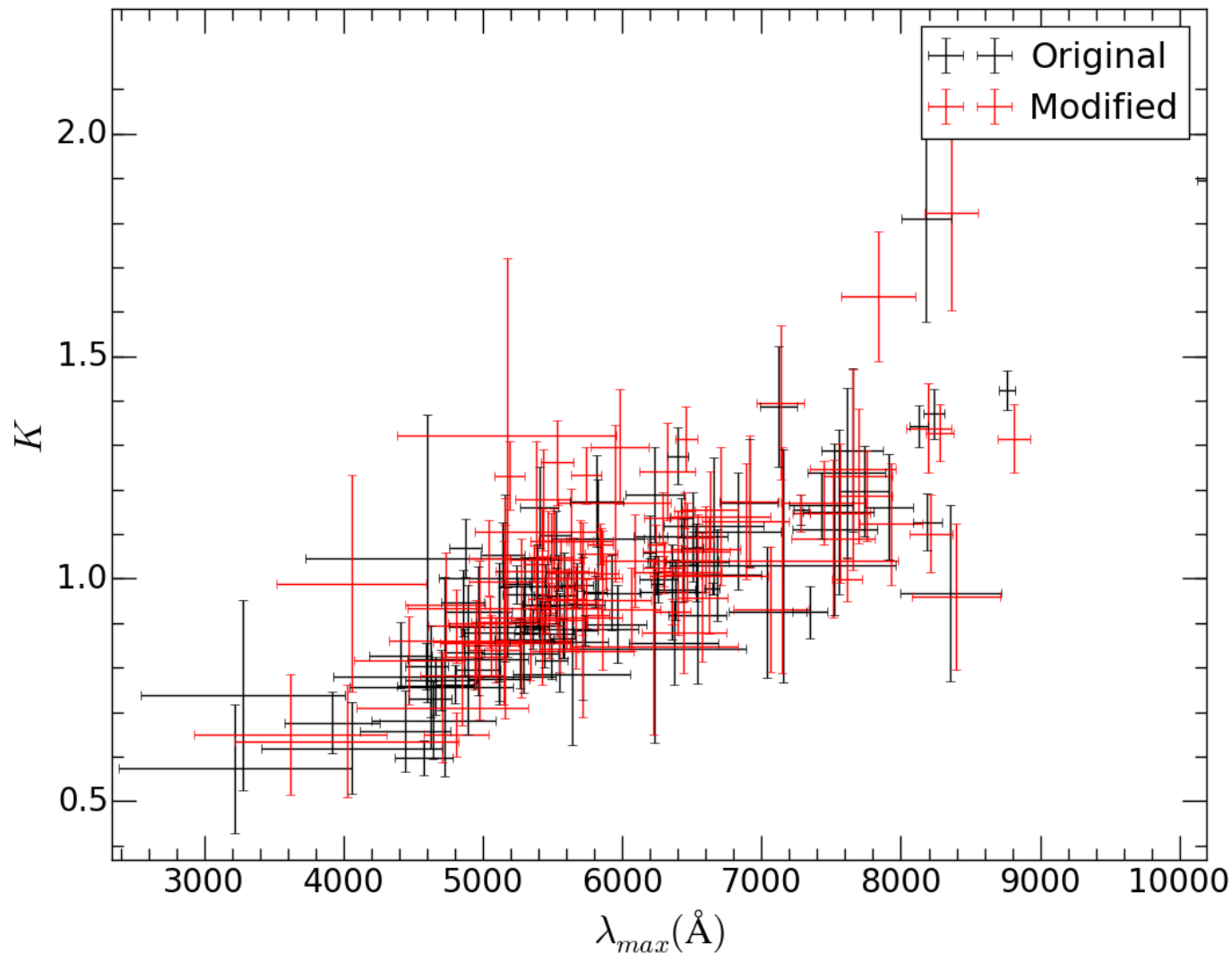




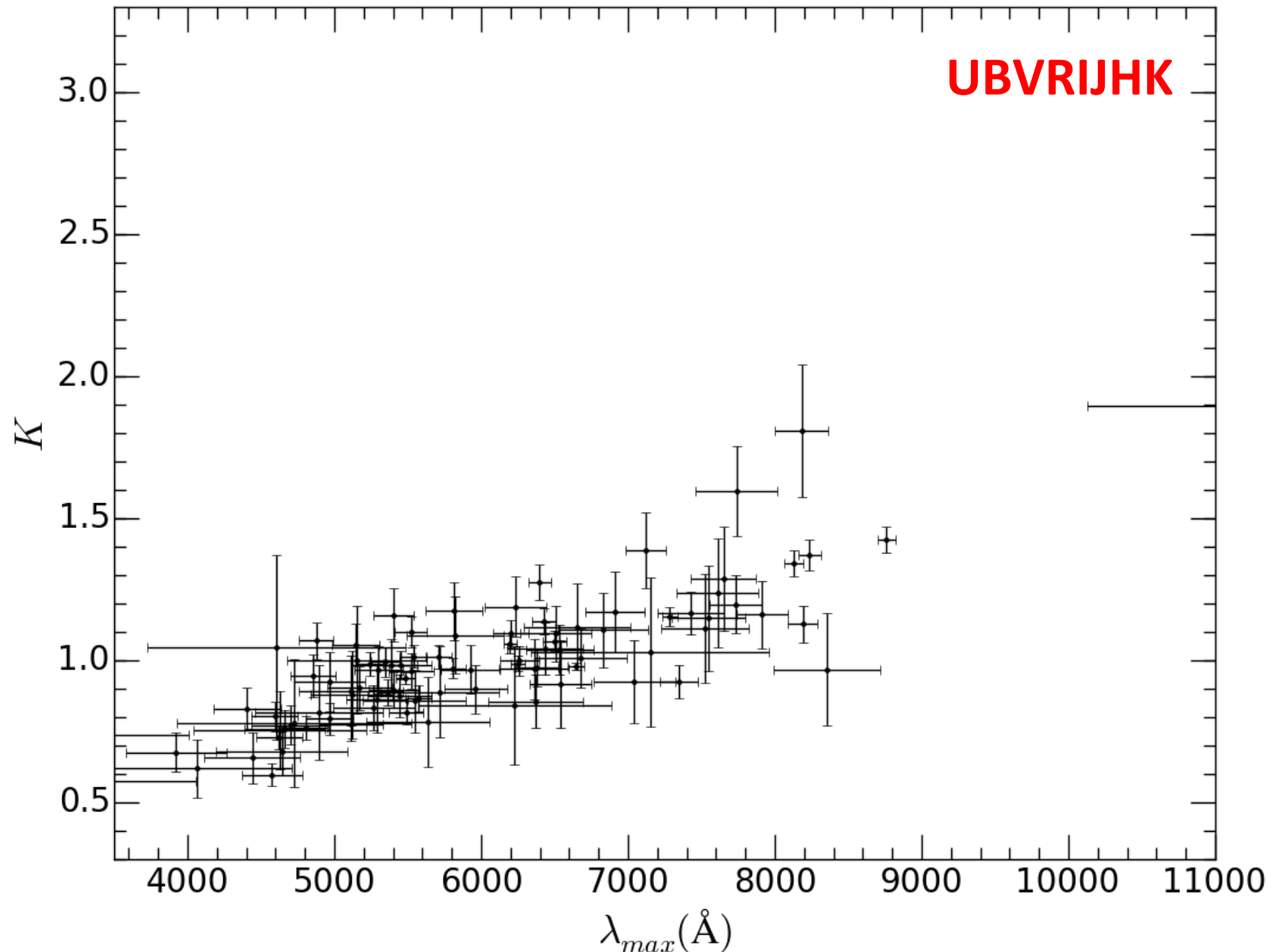




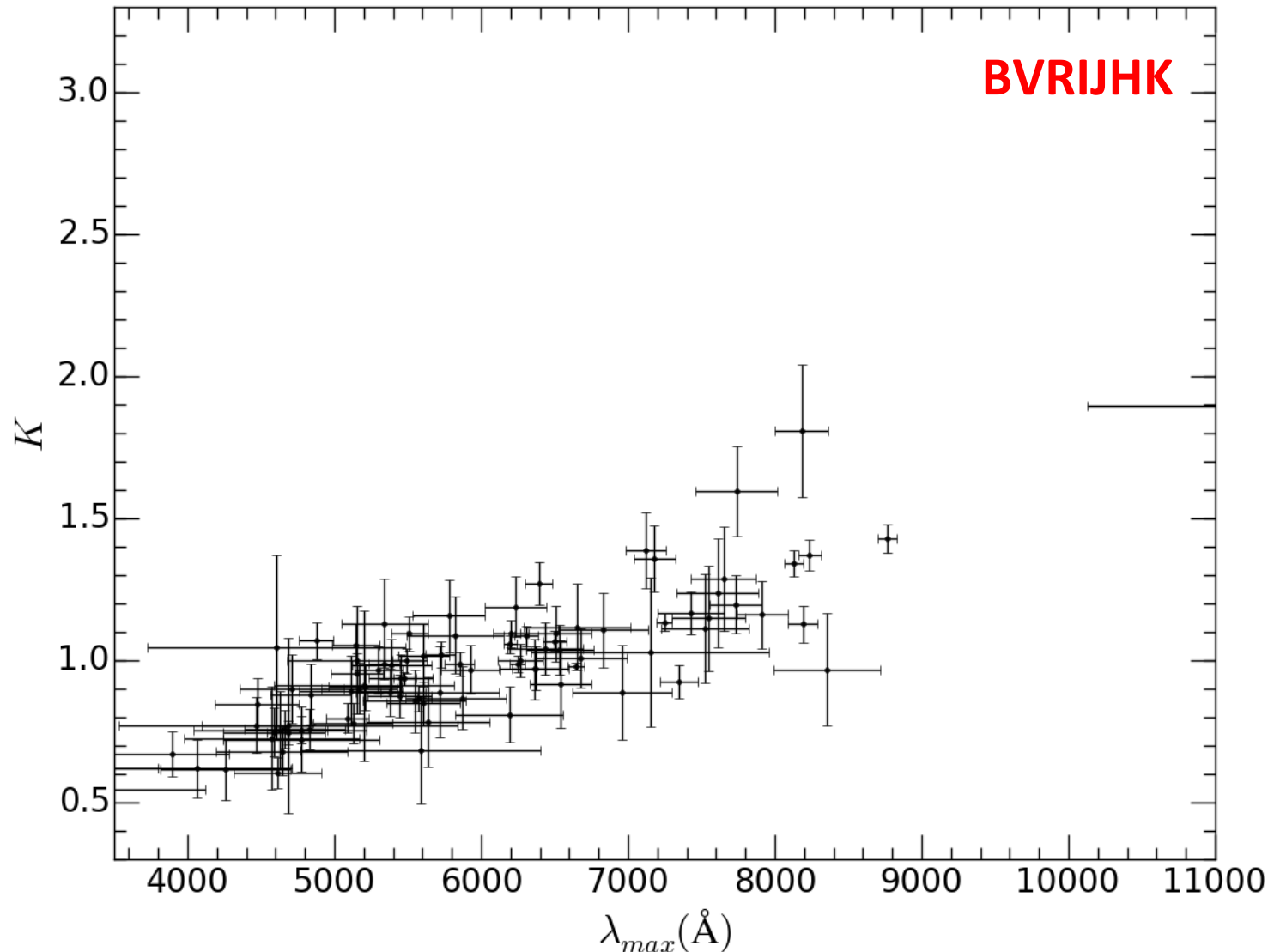
Effect of *R*/ passband wavelengths



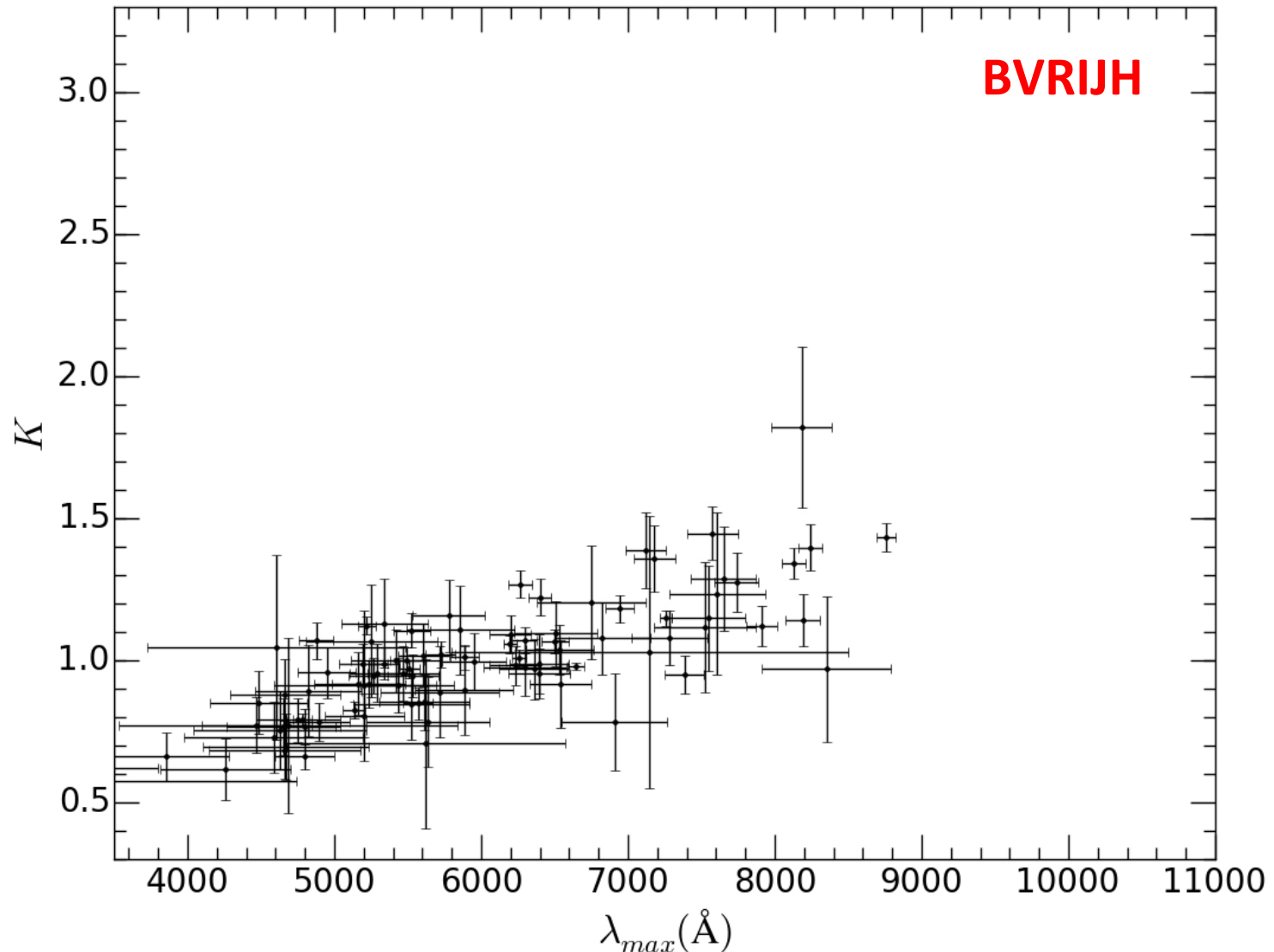
Effect of observed wavelength range



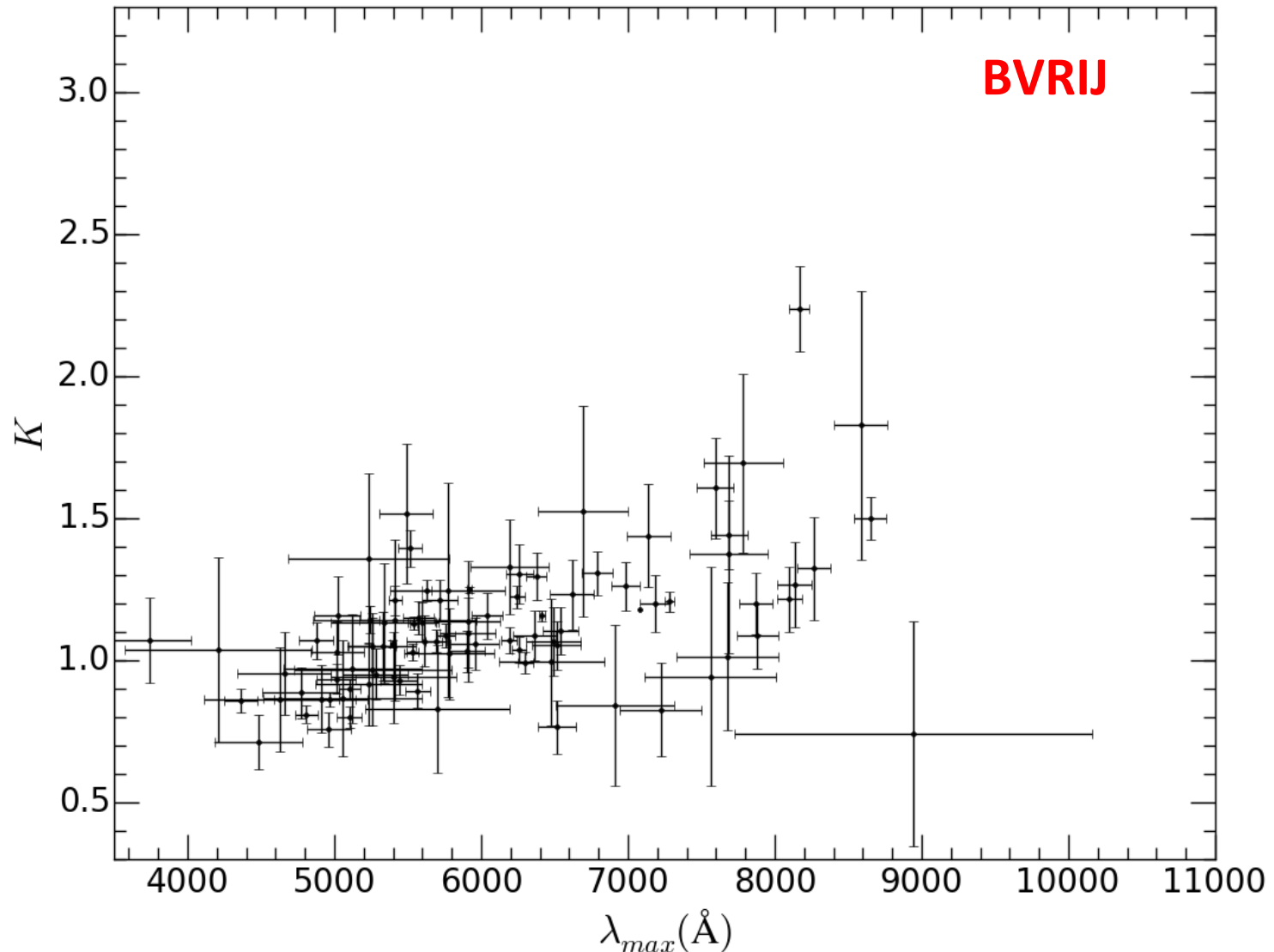
Effect of observed wavelength range



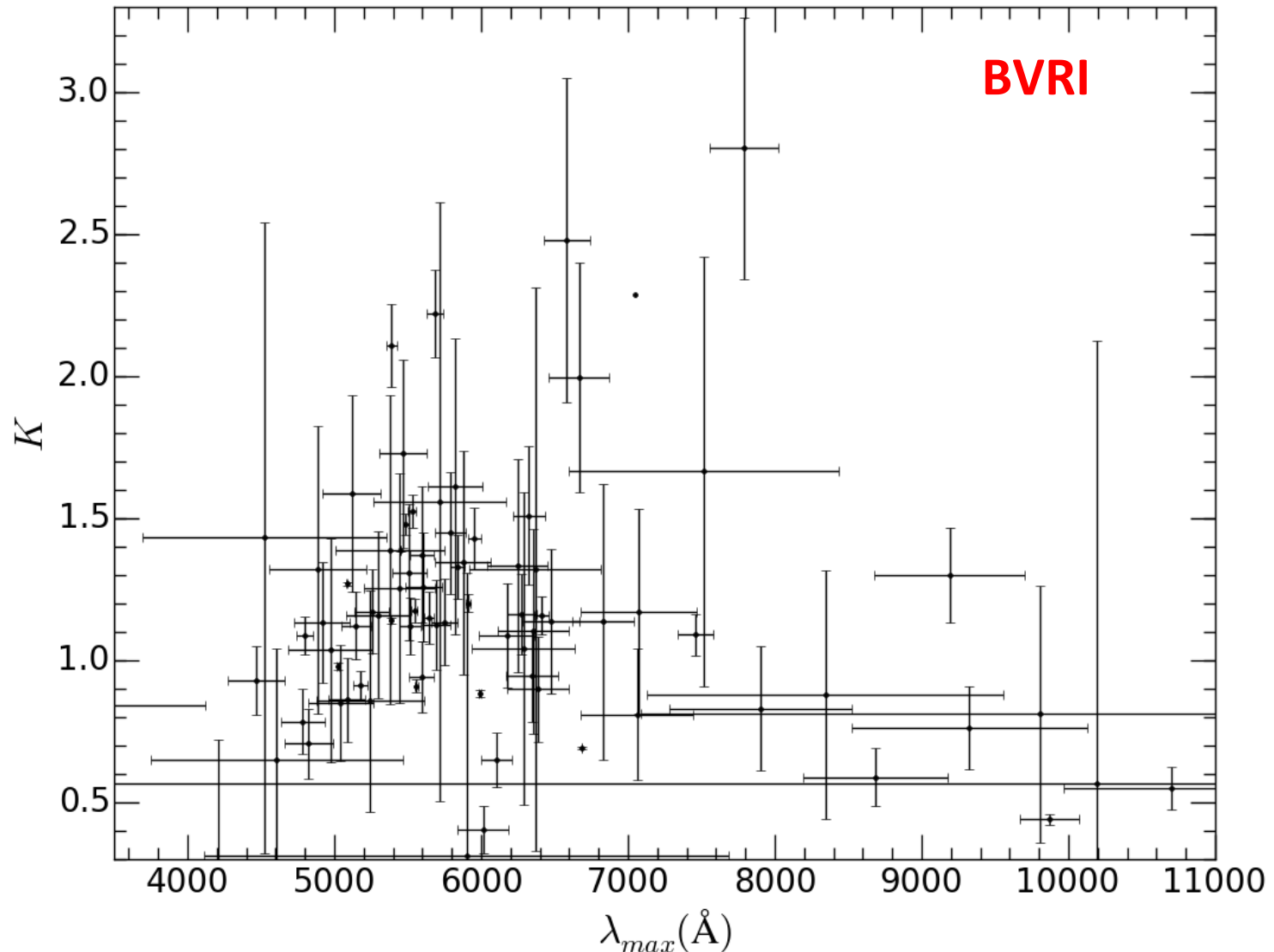
Effect of observed wavelength range



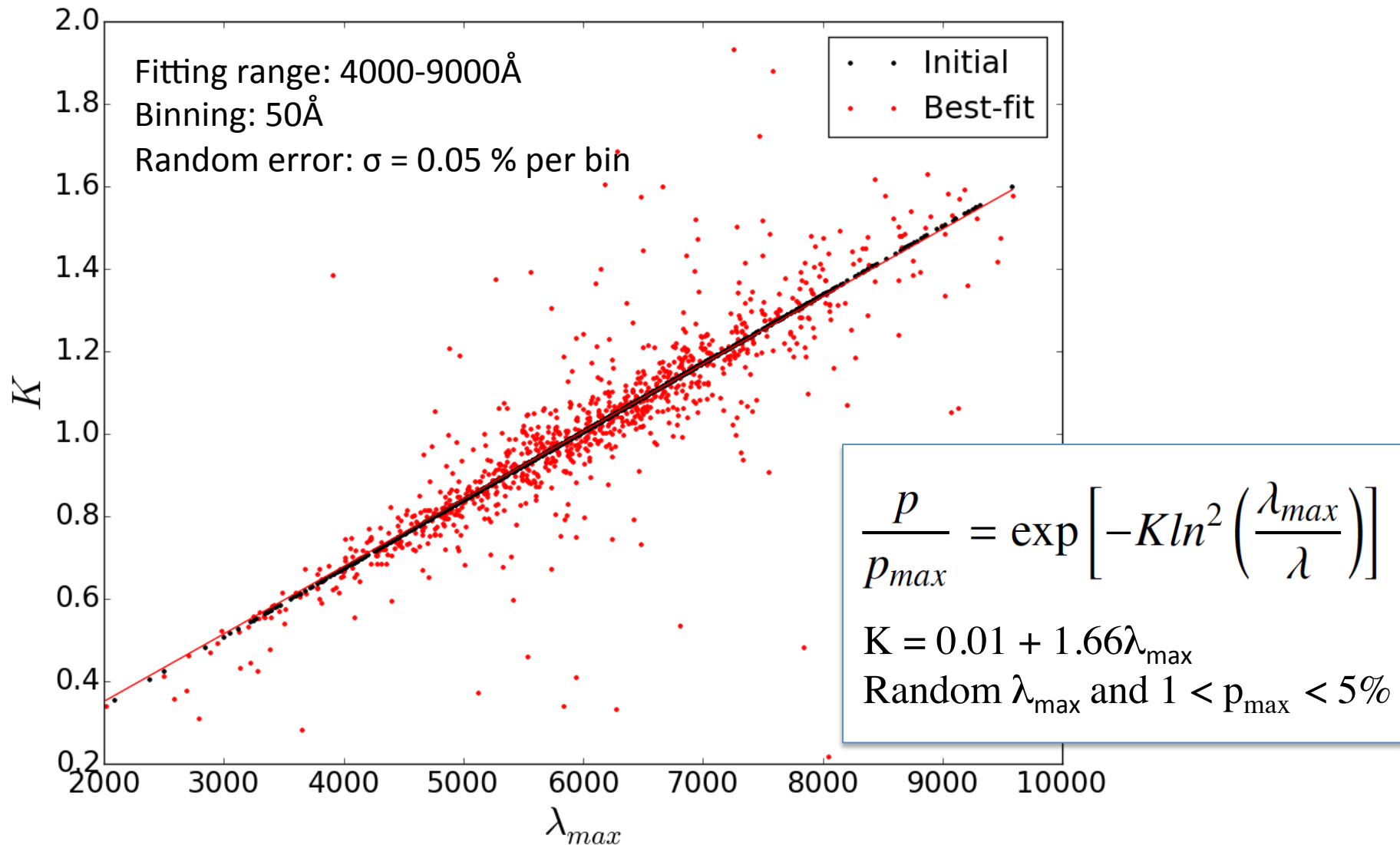
Effect of observed wavelength range



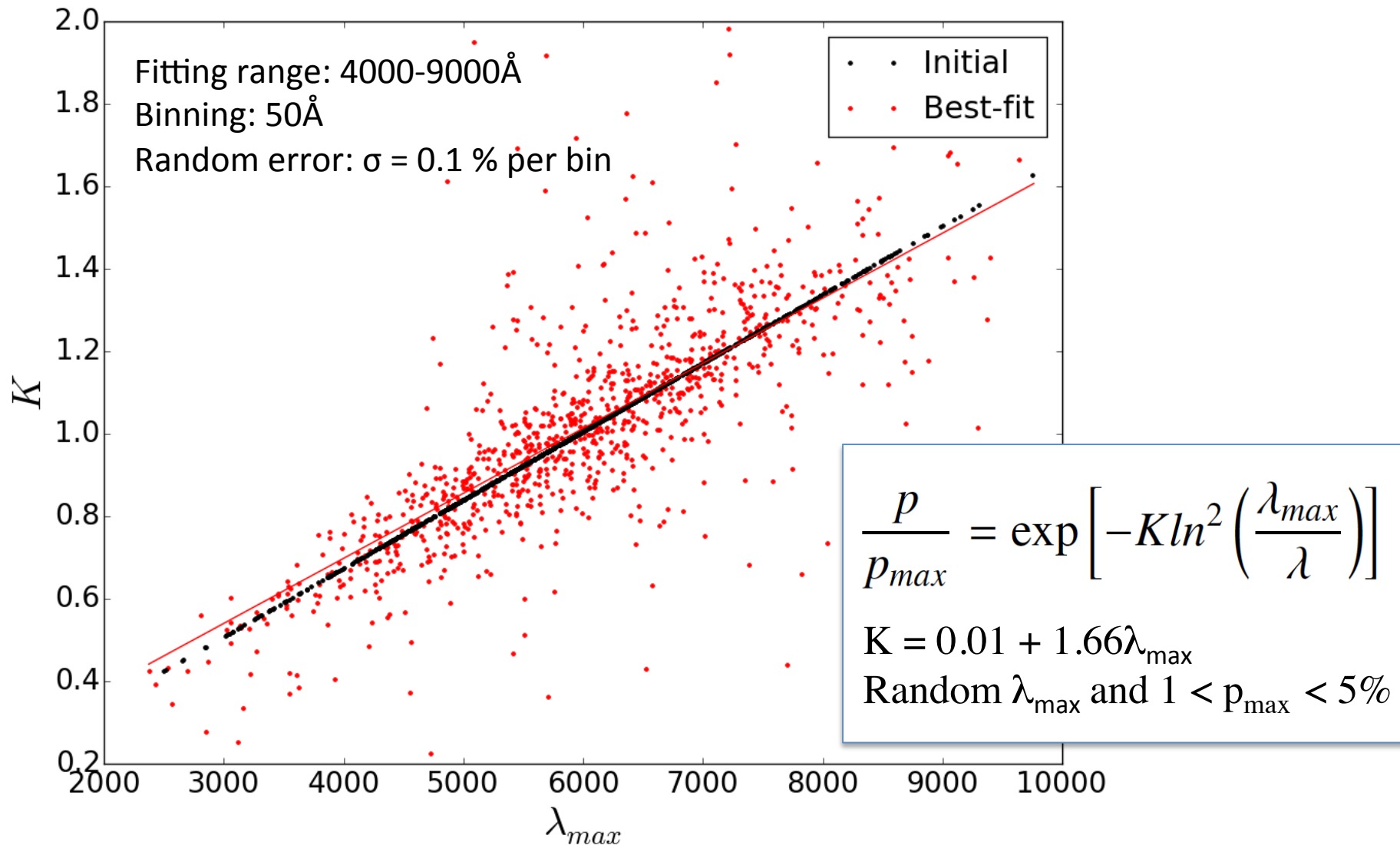
Effect of observed wavelength range

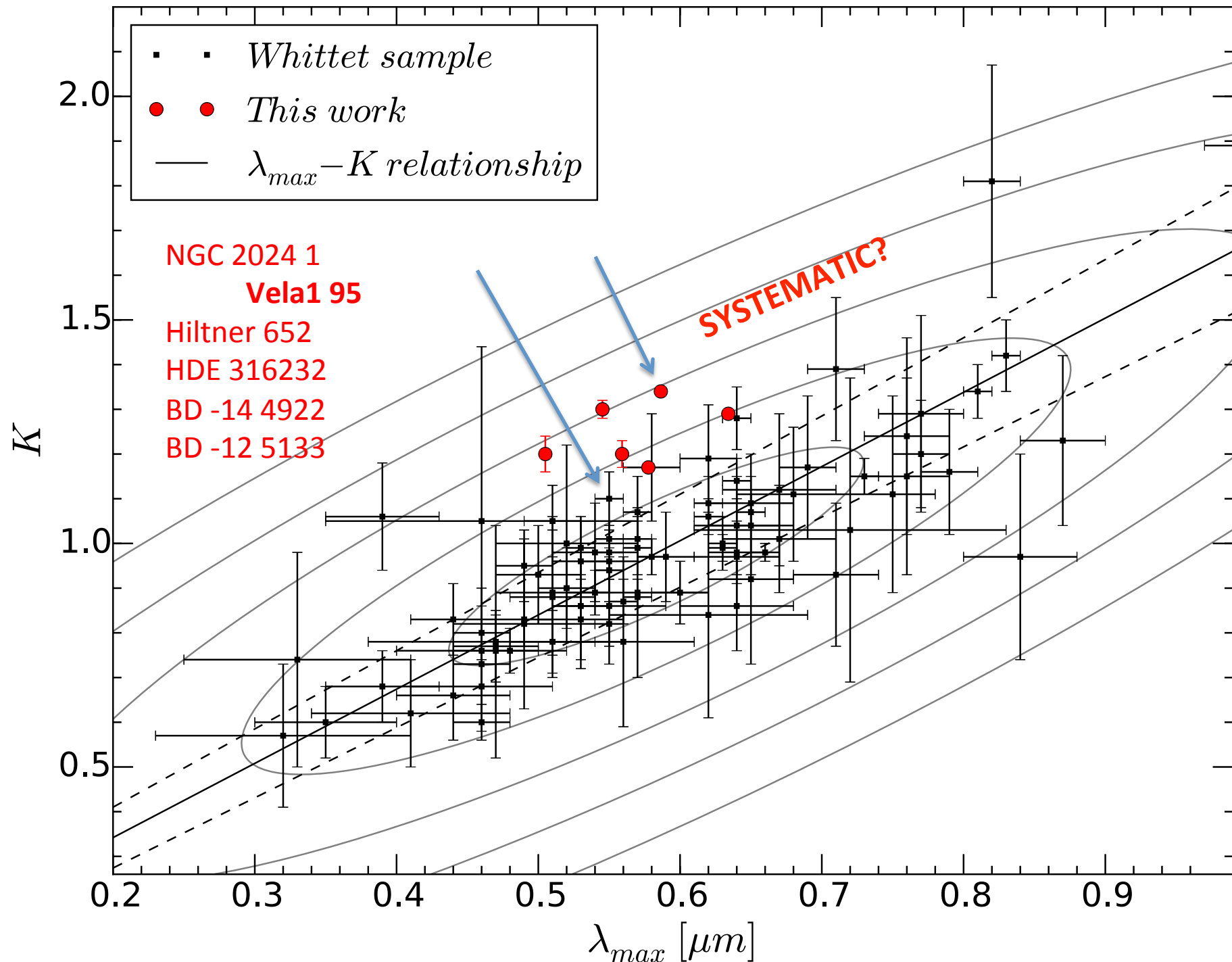


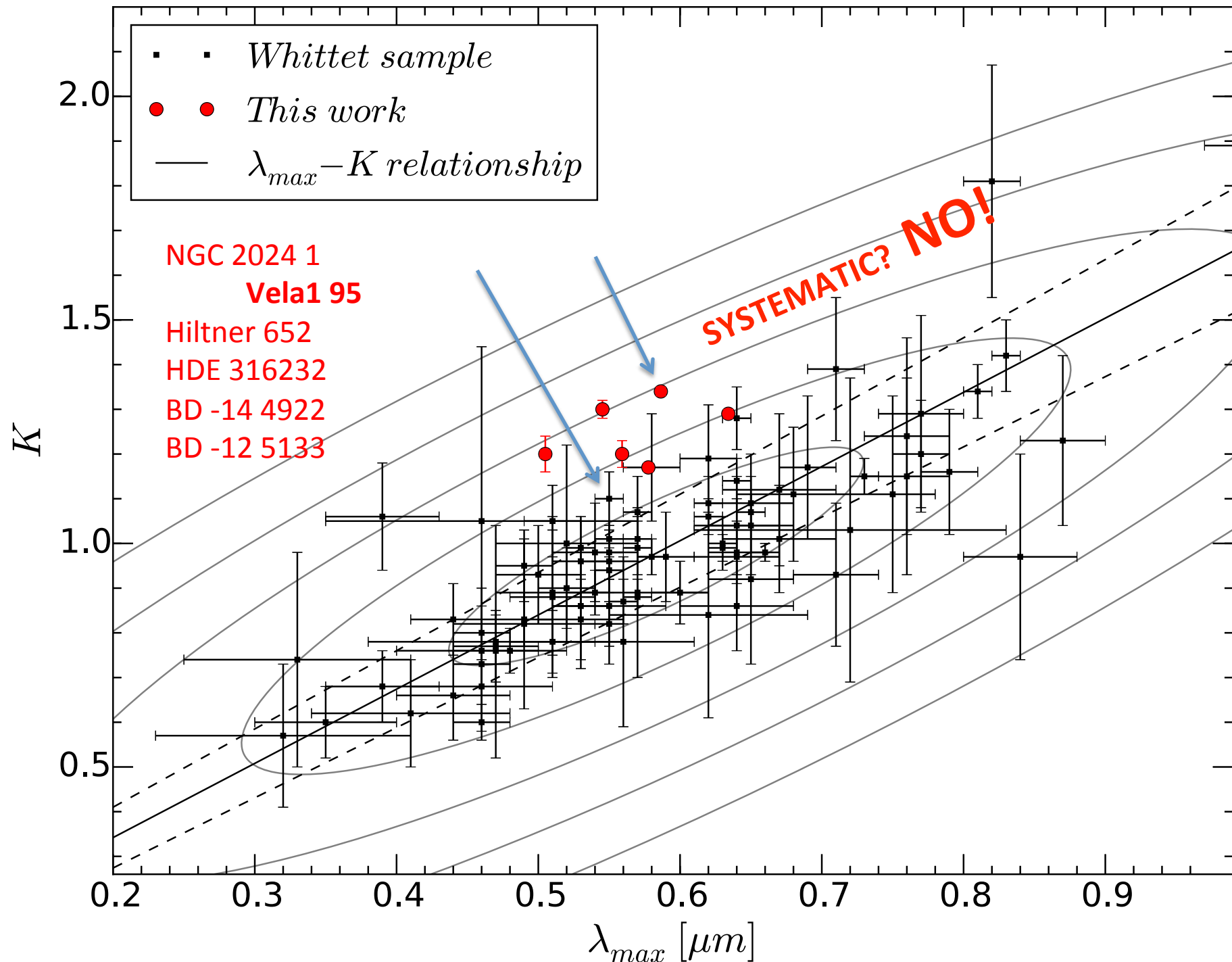
Effect of observed wavelength range



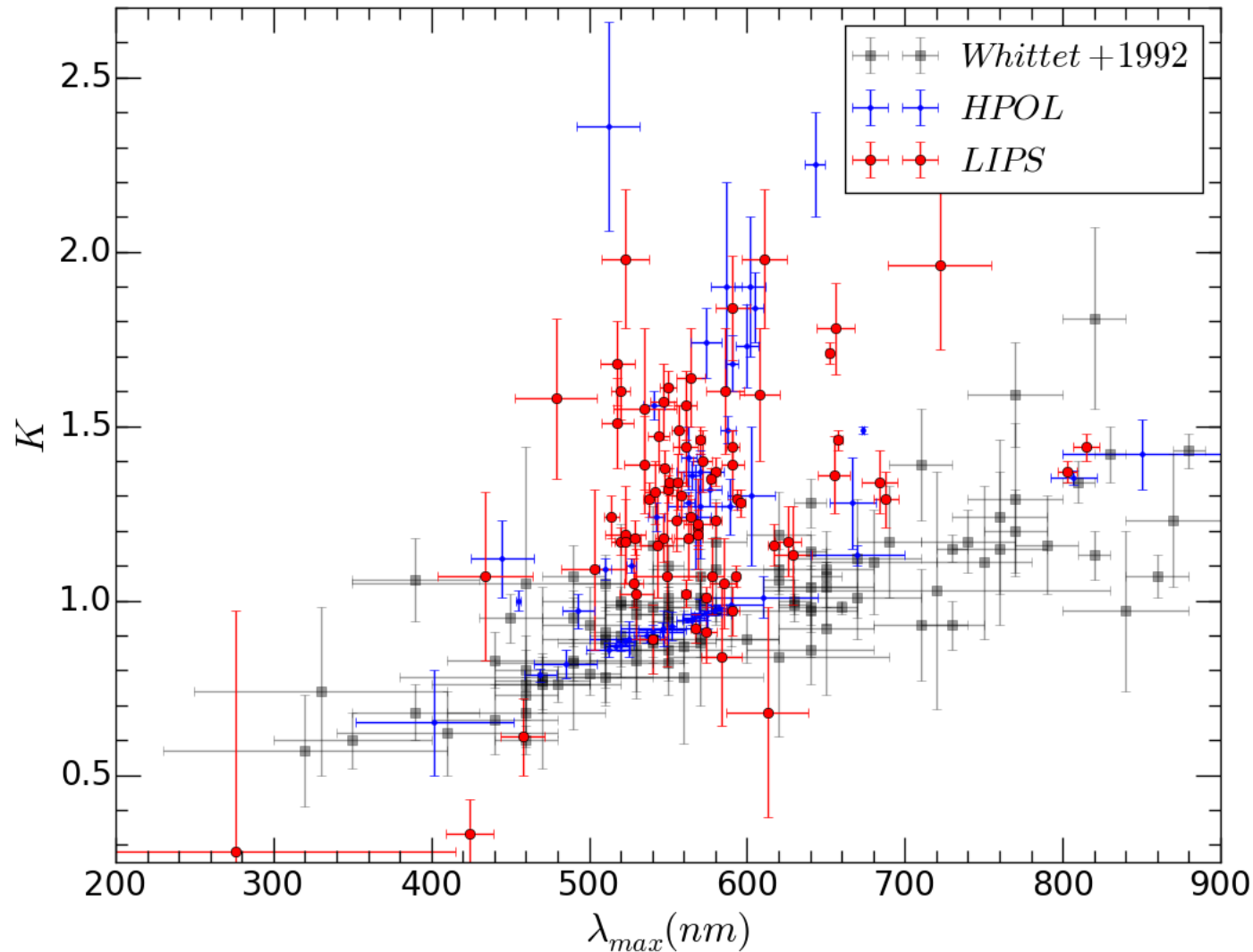
Effect of observed wavelength range



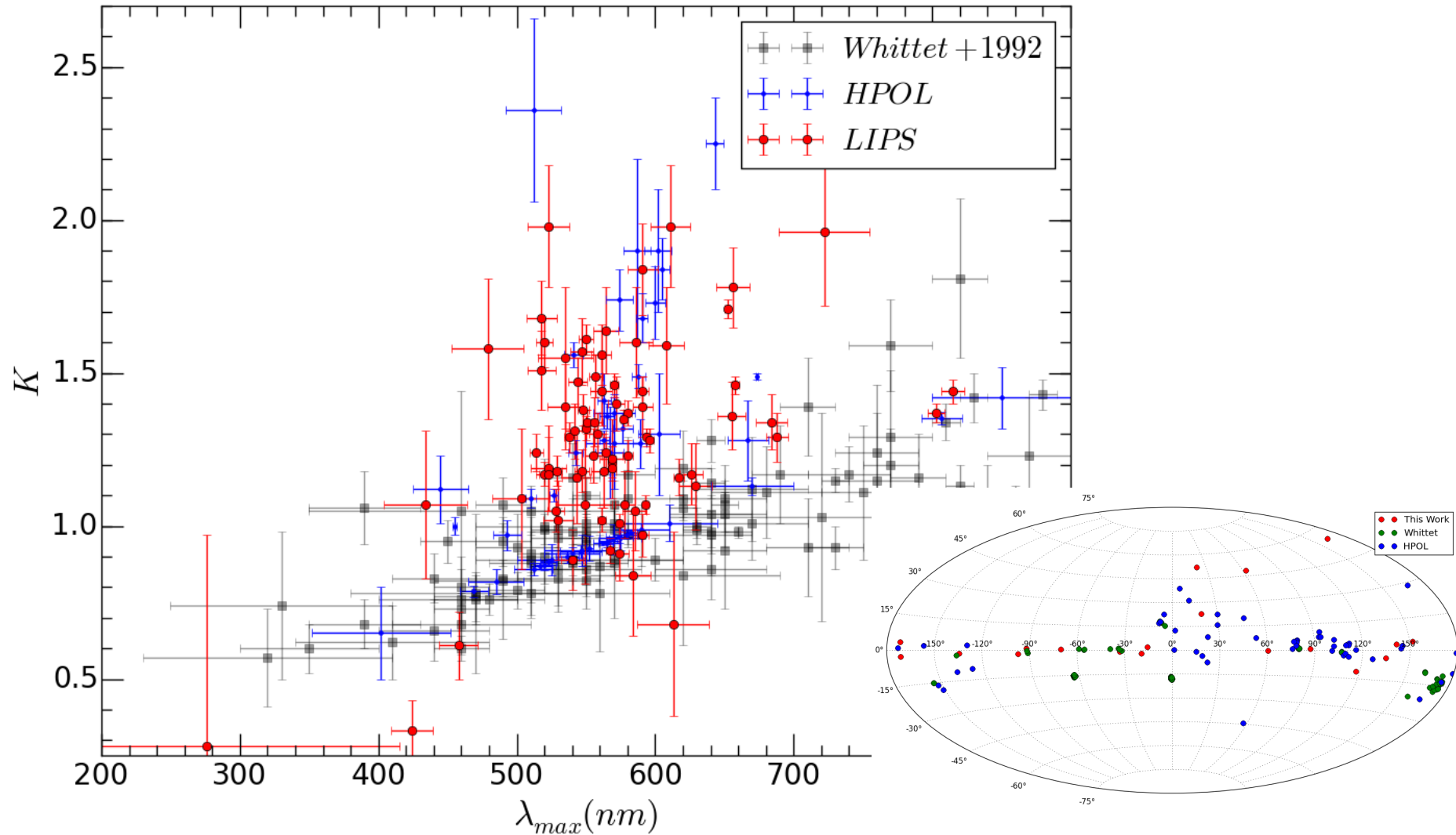




Interpretation of the non-detection of λ_{\max} -K relationship



Interpretation of the non-detection of λ_{\max} -K relationship



Summary and conclusions (1)

- We used archival FORS2 observations of six polarized (30 epochs) and 8 unpolarized (40 epochs) standard stars to characterize the performance and stability of FORS2 mounted at the VLT.
- We confirm the instrumental wavelength dependent polarization detected by Fossati et al. (2007). The spurious signal grows from the blue to the red, ranging from 0.05% (4000Å) to 0.10% (9000Å). The physical cause of this instrumental polarization is still unclear, but it is most likely related to the tilted surfaces of the dispersive element.
- repeatability of total linear polarization spanning 5 years: RMS variation is $\lesssim 0.2\%$. For comparison, the typical error per 50Å bin for a single epoch is $\lesssim 0.1\%$.
- HWP positioning stability: RMS = 0.27° . For comparison, the typical uncertainty in the weighted mean is $\sigma_\theta \lesssim 0.05^\circ$, while the typical uncertainty per 50Å bin for a single epoch is $\lesssim 0.5^\circ$.

Summary and conclusions (2)

- We simulated the effect of HWP positioning inaccuracy:
0.1 degree inaccuracy \rightarrow $\sim 0.03\%$ in polarization
- Our polarization results are in good agreement with those reported in the literature. Peak polarization (P_{\max}), peak wavelength (λ_{\max}) and width parameter (K) were determined via least squares fit of the classical Serkowski law to the observed data.
- Given the larger telescope size and the superb performance of FORS2, the data presented in Cikota et al. 2016 provide a robust re-calibration that can be reliably used for both checking the performance of other polarimeters and calibrating scientific data obtained with those instruments

Thank you!

Contact:

acikota@eso.org

<http://www.eso.org/~acikota>

Literature

- Cikota et al., 2017, MNRAS, 464, 4146
- *Very Large Telescope*. Paranal Science Operations. FORS2 User *Manual*. Doc. No. VLT-MAN-ESO-13100-1543. Issue 96.0, Date 24/02/2015
- https://www.eso.org/sci/facilities/eelt/science/doc/SC_EELT_polarimetry_072009.pdf
- <http://image.slidesharecdn.com/nomarskidic-121111051653-phpapp02/95/nomarski-dic-5-638.jpg?cb=1352611081>
- <http://www.dailygalaxy.com/.a/6a00d8341bf7f753ef01a3fd05c1ef970b-pi>